The authors aim to continually improve this manual and encourage your thoughts and recommendations.

Fast Repetition Rate (FRR) Chlorophyll *a* Fluorescence Induction Measurements

David J. Suggett[1], C. Mark Moore[2], Kevin Oxborough[1] & Richard J. Geider[1]

[1] Department of Biological Sciences, University of Essex, Colchester, CO4 3SQ, UK.

[2] Southampton Oceanography Centre, Empress Dock, Southampton, SO14 3ZH, UK.

Acknowledgements

We are indebted to numerous colleagues for their contribution to aspects of this manual in the form of detailed discussion, guidance and collaboration over recent years. In particular, Ed Abraham, Jim Aiken, Marcel Babin, Neil Baker, Phil Boyd, John Cullen, Patricia Estévez Blanco, Paul Falkowski, Rod Forster, Max Gorbunov, Andrés Gutierrez, Yannick Huot, Zbigniew Kolber, Jacco Kromkamp, Sam Laney, Hugh MacIntyre, Ondřej Prášil and Heidi Sosik. As a result, this document has been influenced by several years of FAST^{tracka} Fast Repetition Rate fluorometer (FRRf) usage, experimentation and discussion by an international scientific community throughout numerous laboratory and field programmes. However, the opinions expressed are the authors and we invite both comment and criticism.

This manual is not meant as a complete and comprehensive literature review (although we hope we have covered the most recent and relevant literature available) but more a guide which new users can follow to limit the caveats frequently encountered during a steep FRRf learning curve. Furthermore, we intend that this be a working document open to suggestion, comment and revision from experienced users. We hope that this manual continually captures the current level of our understanding as the use of FRR and other fluorescence induction techniques further expands for both research and monitoring of algae. Preparation of this manual was made possible through NERC funding to RJG/DJS (NER/A/S/2000/01237) and CMM (NER/A/S/2001/00449).

Front Page Picture Credit: David J. Suggett.

Correspondence: David J. Suggett (dsuggett@essex.ac.uk)

Contents

Parameter	Definition	Units
k_f	Probability of de-excitation of absorbed light by fluorescence	Dimensionless
k_p	Probability of de-excitation of absorbed light by photochemistry	Dimensionless
k_h	Probability of de-excitation of absorbed light by heat	Dimensionless
k_s	Probability of de-excitation of absorbed light by spill over	Dimensionless
k_{PQ}	Probability of de-excitation of absorbed light by plastoquinol	Dimensionless
F_o	Minimum fluorescence in darkness	Dimensionless
F_m	Maximum fluorescence in darkness	Dimensionless
F_v	Variable fluorescence in darkness ($F_m - F_o$)	Dimensionless
F_v/F_m	Maximum photochemical efficiency	Dimensionless*
σ_{PSII}	Effective absorption cross section in darkness	$Å^2$ (quanta)$^{-1}$
ρ	Connectivity between PSII reaction centres in darkness	Dimensionless
τ_{PSII}	Minimum turnover time of PSII photochemistry	s^{-1}
F'	Steady state fluorescence at any point	Dimensionless
F_o'	Minimum fluorescence under actinic light	Dimensionless
F_m'	Maximum fluorescence under actinic light	Dimensionless
F_v'	Variable fluorescence under actinic light ($F_m' - F_o'$)	Dimensionless
F_q'	Difference between F_m' and F' ($F_m' - F'$)	Dimensionless
F_q'/F_m'	Photochemical efficiency under actinic light	Dimensionless*
F_q'/F_v'	PSII efficiency factor under actinic light	Dimensionless*
F_v'/F_m'	Maximum PSII efficiency under actinic light	Dimensionless*
σ_{PSII}'	Effective absorption cross section under actinic light	$Å^2$ (quanta)$^{-1}$
ρ'	Connectivity between PSII reaction centres under actinic light	Dimensionless
τ_{PSII}'	Minimum turnover time of PSII photochemistry	s^{-1}
p	Proportion of 'open' PSII reaction centres	Dimensionless
PPFD (=E)	Photosynthetically active photon flux density	μmol m^{-2} s^{-1}
n_{PSII}	Photosynthetic unit size of PSII reaction centres	mol RCII mol chla^{-1}
$1/k$	Maximum yield of O_2 from each electron transfer step through PSII	mol O2 (mol e^-)$^{-1}$
$ETR^{RCII\ (chl)}$	RCII (Chlorophyll *a*)-normalised rate of electron transfer by PSII	mol e^- mol RCII^{-1} h^{-1} mol e^- g chla^{-1} h^{-1}
PO_2	RCII (Chlorophyll *a*)-normalised rate of potential PSII O_2 production	mol O_2 mol RCII^{-1} h^{-1} mol O_2 g chla^{-1} h^{-1}
a^{chl}_{PSII}	a^{chl} only used for PSII photochemistry	m^2 mg chla^{-1}

Table 1. Terms and definitions used for fluorescence-based techniques (taken from Baker & Oxborough 2003, Kromkamp & Forster 2003). Note all fluorescence parameters are specific to the protocol used and can be followed by ST or MT to denote single or multiple turnover yields (Kromkamp & Forster 2003).* indicates that although strictly dimensionless the parameter defines the efficiency that absorbed photons are used for linear electron flow and can be expressed as mol e^- mol photons^{-1}.

A. Background

Fluorescence has been used to assess changes in the abundance of phytoplankton since the 1960s (Lorenzen 1966). Fluorescence is the emission of light at a longer wavelength that occurs after light absorption at a shorter wavelength. The fluorescence that arises from chlorophyll *a* provides a rapid, sensitive, non-destructive measurement of algae that can be readily assimilated into environmental monitoring and assessment programmes, such as detection of coastal eutrophication.

Recent technological advances have significantly increased the availability of a variety of fluorometers to many user groups. Fluorescence measurements have become routine for many algal research and monitoring programmes. However, both the variety of fluorometers that are available and the actual fluorescence measurements themselves have meant that fluorescence data collected from natural microalgal populations are difficult to interpret. Furthermore, data collected from different sampling campaigns or experiments are difficult to inter-compare. This manual provides a brief overview of the operating principles and suggested protocols for a fluorescence induction technique known as Fast Repetition Rate fluorometry (FRRf, Kolber et al. 1998) with specific reference to a commercial FRR fluorometer manufactured by the *Chelsea Technologies Group*, the FAST$^{tracka™}$ FRRf.

1. In vivo fluorescence for estimating phytoplankton abundance— When pigments are extracted in solvents such as acetone or methanol, the fluorescence that arises is referred to as *in vitro* fluorescence. A one-to-one relationship is expected between the *in vitro* fluorescence and the concentrations of the pigments in the sample (the chlorophylls and their breakdown products). This simple relationship does not hold for the *in vivo* fluorescence of intact cells. When *in vivo* and *in vitro* fluorescence are measured on the same sample, the ratio of fluorescence to chlorophyll a can be calculated. This ratio varies by about a factor of 20, with most of the variability due to the taxonomic composition of the sample, although the physiological condition of the sample can also be significant. Thus, *in vivo* chlorophyll fluorescence does not provide an absolute measurement of the amount of chlorophyll *a* in a water sample. However, changes of *in*

vivo fluorescence can be used to infer changes in phytoplankton abundance, although care must be taken in the interpretation of any changes that are observed.

A number of factors contribute to the measured *in vivo* fluorescence. These are the

- wavelength used to illuminate (excite) the sample,
- wavelength at which fluorescence emission is measured,
- intensity of the excitation beam,
- concentration of chlorophyll *a* in the sample
- chlorophyll-specific light absorption coefficient,
- proportion of absorbed light that is transfered to photosystem II
- quantum yield of fluorescence.

The actual i*n vivo* fluorescence that is measured is dependent upon the wavelength used for excitation. Most fluorometers deliver narrow-band blue light to correspond with wavelengths at which phytoplankton exhibit maximum rates of light absorption. Subsequent detection of fluorescence is centred at 680 nm to correspond with the peak chlorophyll *a* emission from photosystem II. Therefore, fluorescence excitation and emission is inherently tied to the optical properties of the fluorometer, natural light absorbed and the phytoplankton in question.

2. Fluorescence Induction = Variable Fluorescence— Fluorescence induction is now routinely employed to investigate aspects of algal physiology (Kautsky et al. 1960), where variations in fluorescence emission are measured in response to variations in excitation energy. Commercial availability of induction fluorometers has meant that the use of fluorescence in aquatic research has grown substantially in the last 10 to 15 years, although the theoretical basis for the application of these techniques dates to the 1960s. Of key interest to many researchers is the use of fluorescence to assess aquatic primary production free from constraints that exist using more conventional techniques, such as O_2 evolution or ^{14}C uptake (Falkowski & Kiefer 1985, Kolber & Falkowski 1993, Sakshaug et al. 1997, Laws et al. 2002). However, synthesis of information gained from fluorescence techniques, particularly for the novice, is hampered by (1) variations in the protocols to induce variable fluorescence and (2) use of different terminology for describing equivalent (or nearly equivalent) fluorescence measurements.

3. The fluorescence Yield, F— The fluorescence yield that arises from an excitation light source is typically referred to as *F* and is often expressed in instrument units (ultimately as V or mV). The optical geometry of the measurement system comprising the excitation light source, sample compartment and detector will affect the fluorescence yield that is measured. Typically, fluorescence is measured in relative units, although for a given optical geometry, *F* will vary with the absorbtivity (A) of the sample and the photosynthetic photon flux density (PPFD) of the excitation light source,

$$F = \phi_F \cdot C \cdot \mathrm{A} \cdot \mathrm{PPFD}$$

where *F* is the fluorescence signal, A is the absorbtivity of the sample, ϕ_F is the quantum yield of fluorescence, PPFD is the photosynthetic photon flux density, and *C* is a constant that accounts for the optical geometry of the measurement system. Specifically, the value of *C* depends on the proportion of fluoresced light that is intercepted by the detector and the efficiency of conversion of photons into an electric signal.

Fluorescence may be measured in darkness or under actinic illumination. When measured in darkness, the light source used to excite the fluorescence signal must be of a sufficiently low PPFD that photosynthesis does not take place (i.e., the light source must not affect the redox state of any of the components of the photosynthetic electron transfer chain).

4. ***Variable fluorescence—*** Measurements of variable fluorescence are interpreted in terms of theoretical constructs (Butler 1978, Lavernge and Trissl 1995). These models consider how changes in the quantum (photon) yields of competing processes affect the quantum yield of fluorescence. In practice, absolute quantum yields are not measured, nor do they need to be, provided that the fluorescence signals that are measured accurately report changes in the relative quantum yield of fluorescence. Thus, it is assumed that changes in the fluorescence variables (Table 1) accurately reflect changes in the absolute quantum yields.

In chlorophytes and chromophytes, most of the fluorescence measured at room temperature arises from photosystem II (e.g., 99% at the emission peak at 680 nm). For the moment, we will assume that fluorescence emission by other processes is minimal and can be neglected.

The analysis of the relationship between fluorescence and the photon efficiency of photosynthesis assumes that fluorescence is one of four pathways for the deactivation of excitation energy absorbed by photoautotrophs. The other pathways are photochemistry, spillover to PSI and thermal de-excitation (Fig. 1).

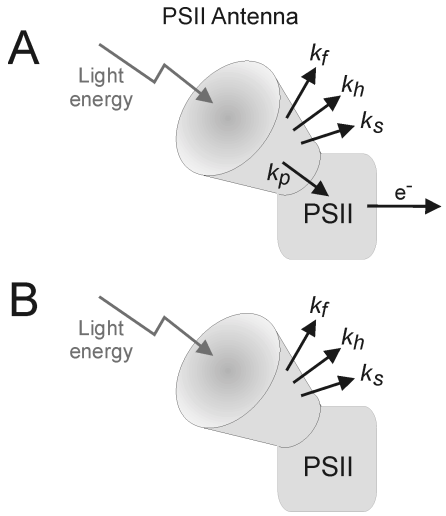

$$k_f + k_h + k_s + k_p = 1$$

$$k_f + k_h + k_s = 1$$

Figure 1. Schematic dissipation of absorbed light by PSII when reaction centres are (A) available to receive excitation energy (B) 'closed' to further excitation. The probability (k) that incident light energy is dissipated by heat ($_h$), photochemistry ($_p$), spill-over ($_s$) and fluorescence ($_f$), is equal to 1. When reactions centres are closed, k_p is reduced to zero whilst the probability by all other pathways, in particular k_h, are increased.

The fluorescence emitted from algae can be related to the photosynthetically active photon flux density (PPFD) of an excitation light source and the light absorption coefficient (A) through the rate constants for the fluorescence (k_f), photochemistry (k_p), heat production (k_h) and spillover to photosystem 1 (k_s) and the proportion of PSII reaction centres that are open (p),

$$F = \frac{k_f}{k_f + k_h + k_s + (1-p)k_p} \cdot \mathrm{PPFD} \cdot A$$

The maximum quantum efficiency of photosystem II photochemistry can be obtained from measurements of fluorescence made when samples are manipulated such

that p is either made equal to zero or unity. When $p = 0$, all reaction centres are said to be 'open' and ready to receive excitons, and the minimum fluorescence yield, F_o, is measured,

$$F_o = \frac{k_f}{k_f + k_h + k_s + k_p} \cdot \text{PPFD} \cdot A$$

In contrast, when $p = 1.0$, all reaction centres are closed and the maximum fluorescence yield, F_m, is measured,

$$F_m = \frac{k_f}{k_f + k_h + k_s} \cdot \text{PPFD} \cdot A$$

The photochemical efficiency of PSII is equal to the probability that de-excitation occurs via photochemistry relative to all other pathways. Butler showed that this efficiency can be calculated from the rate constants k_p, k_f, k_h and k_s and, therefore, F_o and F_m,

$$PSII\ photochemcial\ efficiency = \frac{k_p}{k_f + k_h + k_s + k_p} = \frac{F_m - F_o}{F_m}$$

In addition to the assumption that all fluorescence arises from PSII, this analysis also assumes that the rate constants are not affected by the measurement protocol. As we will see in the next section, this assumption is not always valid.

5. ST versus MT maximum fluorescence— The fast repetition rate fluorometer (Kolber et al. 1998), which builds on an earlier pump and probe technique (Falkowski et al. 1986, 1988, Kolber and Falkowski 1993), delivers a rapid chain of flashes of ~ 27500 μmol photons m^{-2} s^{-1} over a period of 150-400μs to obtain F_m. This method allows a simultaneous, single turnover (ST) of most PSII reaction centres. In contrast, other commercially available fluorometers, for example, pulse amplitude modulation fluorometer (*Walz*, Schreiber et al. 1993, 1995a, b) use a prolonged duration of saturating

light and induce multiple photochemical turnovers (MT) of individual PSII reaction centres (Fig. 2). The ST method typically provides lower values of F_m than the MT technique (Schreiber et al. 1995a, b, Prasil et al. 1996, Kolber et al. 1998, Koblízek et al. 2001, Suggett et al. 2003, Gorbunov and Falkowski 2004). This implies that at least one of the rate constants differs between ST and MT measurements of F_m. The explanation for this difference is thought to reside in the difference in the redox state of the plastoquinone pool that is induced by the two techniques.

The ST technique fully reduces the pool of Q_A but has minimal effect on the redox state of the plastoquinone pool (PQ). In contrast, the MT technique fully reduces Q_A and in addition further reduces plastoquinone to plastoquinol. Plastoquinone is a quencher of chlorophyll fluorescence while plastoquinol is not and the maximum fluorescence measured using multiple turnover increases as plastoquinone is reduced to plastoquinol (eg. Vernotte et al. 1979). This difference in F_m between ST and MT

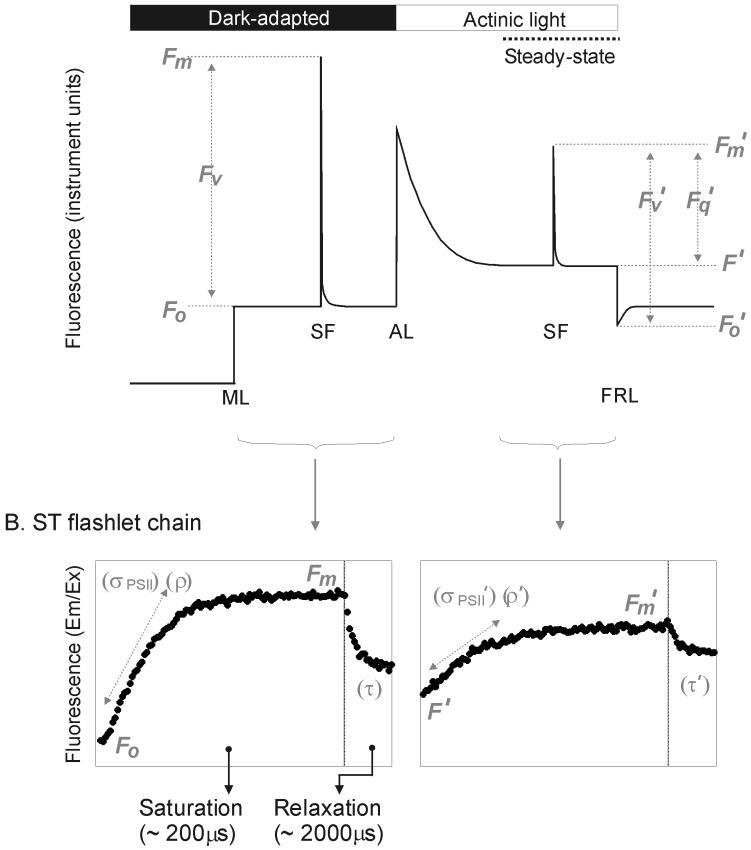

Figure 2. Multiple turnover (MT) and single turnover (ST) fluorescence induction techniques employed by the Pulse Amplitude Modulation and FRR fluorometers, respectively. Examples are shown for phytoplankton in the dark (dark-adapted) and under actinic light. (A) The MT technique delivers a single high intensity saturating flash. (B) The ST technique delivers a series of sub-saturating flashlets. The interval between flashlets is altered to examine the saturation and relation kinetics of photosystem II. All symbols are described in Table 1 except ML (modulating light), SF (saturating flash), AL (actinic light) and FRL (far-red light).

techniques can be clarified by employing the terminology F_m^{ST} or F_m^{MT} (Koblízek et al. 2001, Kromkamp & Forster 2003).[1]

An additional rate constant can be introduced to specify the dissipation of excitation energy associated with PQ quenching (k_{PQ}). k_{PQ} will equal zero where the MT technique is used to obtain F_m. Neither the ST or MT method affects the redox state of the PQ pool during measurement of F_o and k_{PQ} should be equal for both techniques. Therefore, the PSII photochemical efficiency will be higher when F_m is measured using multiple turnover than single turnover methodology (Schreiber et al. 1995a, b, Kolber et al. 1998).

$$F_o = F_o^{ST} = F_o^{MT} = \frac{k_f}{k_f + k_{PQ} + k_h + k_s + k_p} \cdot \mathrm{PPFD} \cdot A$$

$$F_m^{\mathrm{ST}} = \frac{k_f}{k_f + k_{PQ} + k_h + k_s} \cdot \mathrm{PPFD} \cdot A$$

$$F_m^{\mathrm{MT}} = \frac{k_f}{k_f + k_h + k_s} \cdot \mathrm{PPFD} \cdot A$$

Several processes that act to quench fluorescence are thought to occur in the RCII itself (eg. Falkowski & Raven 1997, Bernhard & Trissl 1999) leading to an overall reduction in the efficiency of PSII photochemistry: These include (1) reverse formation of the original excited P680 (P680*) from the primary radical pair, (2) eventual exciton decay into triplet carotenoids and (3) exciton collision leading to singlet-singlet annihilation. The latter two processes are not thought to be significant at the excitation intensities used by PAM (Bernhard & Trissl 1999) or FRR (Kolber et al. 1998) fluorometry protocols. Therefore, the occurrence of a back reaction to form P680* may predominantly explain why values of the factor $(F_m\text{-}F_o)/F_m$ (= F_v/F_m, Table 1) are always likely to be much less than one (Schatz et al. 1988) using either ST or MT protocols.

[1] Alternatively, F_m obtained where PQ is or is not fully reduced has been expressed as I_2 and I_1, respectively (Schreiber et al. 1995a, b). However, we will follow the terminology of Koblízek et al. (2001).

6. *Fluorescence induction measurements in darkness*— Dark measurements are useful since k_p and k_h are not altered as a result of transient changes in PPFD that may occur. These fluorescence parameters can then be used to determine the maximum photochemical efficiency (F_v/F_m) (section A.4.) and, in the case of FRR fluorescence, the maximum effective rate of light absorption (σ_{PSII}) (Fig. 2). Measurements of F_v/F_m for a particular alga differ when grown under relatively low or high photon flux densities and under limiting or replete nutrient concentrations (Fig. 2). Values of F_v/F_m can also display differences between algal species when grown under similar conditions (Casper-Lindley & Bjorkman 1998, Koblizek et al. 2001) presumably from inter-specific differences in components that comprise k_p and k_h. Measurements of σ_{PSII} also vary for any species grown under different light or nutrient condition and between species (Koblizek et al. 2001, Suggett et al. 2004). This variability is the result of alterations to components that determine light harvesting by PSII, for example, pigment type, pigment organisation and the number of PSII reaction centres fed by the antennae complex (Suggett et al. 2004).

In darkness, one expects PQ to be fully oxidized and k_{PQ} to be highest. However, chlororespiration can occur in darkness thus reducing PQ and lowering k_{PQ}. As a consequence, F_o is expected to be higher in the presence of chlororespiration. Similarly, F_m^{ST} is also expected to be higher in the presence of chlororespiration. In contrast, chlororespiration is not expected to affect F_m^{MT} since PQ is completely reduced by this technique. However, a decline of plastoquinone quenching may not be the only consequence of chlororespiration. Reverse electron flow from PQ may lead to the reduction of Q_A and a lower k_p (Dijkman & Kroon 2002) leading to an increase of F_o. A reduction of Q_A in darkness is particularly evident in prokaryotic photoautotrophs, and is accompanied by a state 2 transition, since these organisms contain a common PQ and cytochrome b_6f pool that must be shared for both photosynthesis and respiration (see Behrenfeld & Kolber 1999). These 'dark effects' lower F_v/F_m and σ_{PSII} from a true dark-acclimated value but can be restored by measuring fluorescence from dark-adapted samples maintained under very weak illumination (eg. 0.1 μmol photons m^{-2} s^{-1}, Baker & Oxborough 2003). The use of far-red illumination may be most appropriate for the oxidation of PSI and reversal of potential state 2 transitions.

Differences in dark measures of FRR fluorescence and F_v/F_m are also observed according to the interval between flashes used to obtain F_m^{ST}. A four period oscillation of fluorescence that corresponds with the oxygen evolving (S-state) cycle is observed when F_m^{ST} flashes are separated by 1 second intervals. This process is not well understood but is not observed when the interval between flashes is extended (eg. >120 s) or under illumination (Kolber et al. 1998). These longer intervals lead to higher values of F_v/F_m but are unlikely to reflect a true dark-acclimated value that would correspond with the four-period cycle associated with photosynthetic oxygen evolution.

7. Fluorescence induction measurements in actinic illumination— Alterations to the rate constants k_h and k_p and k_s give rise to variations in F_o and F_m. The proportion of excitation energy dissipated as heat (k_h) follows changes in transthylakoid (Δ)pH and cycling between different pigment types (xanthophyll cycling) (Krause & Weis 1991, Horton et al. 1996) as well as the amount of non-photosynthetic pigment that comprises the total pigment content for light absorption (eg. Casper-Lindley & Bjorkman 1998). These processes compete with fluorescence as a pathway for the dissipation of excitation energy and, therefore, quench the fluorescence observed. Inactivation or loss of PSII reaction centre activity can occur under excess photon flux density (Vasiliev et al. 1994) or nutrient limitation (Kolber et al. 1988) and result in photoinhibitory quenching processes that affect k_p (Krause & Weis 1991). Spillover to PSI enables state transitions to occur under specific changes to the spectral 'quality' of incident light (see Falkowski & Raven 1997, Baker & Oxborough 2003) and when additional ATP must be generated through enhanced cycling of excitons around PSI (Finazzi et al. 2002).

Fluorescence measured under actinic light is distinguished from fluorescence under dark-adaptation by a different set of parameters, all of which are denoted by prime (′). The terminology used to report fluorescence measured in the light is quite inconsistent in the literature (eg. Baker and Oxborough 2003, Kromkamp & Forster 2003, Appendix I). Maximum and minimum fluorescence under actinic light is expressed as F_o' and F_m', respectively (Fig. 2, Table 1). Under actinic light, the observed fluorescence exceeds F_o' since a proportion of PSII reaction centres will be employed for photochemistry at any given irradiance. The parameter F' is used to describe a fluorescence measurement

between F_o' and F_m'. Other notations, such as F_t and F_s (Appendix I) are equivalent to F' but unnecessarily confusing. The difference between F_m' and F' describes variable fluorescence under actinic light and is denoted as F_q' (Oxborough et al. 2000, Baker et al. 2001). ΔF or $\Delta F'$ (e.g. Gorbunov et al. 2000, 2001) have been used as equivalent to F_q' but is an imprecise term that may apply to the difference in fluorescence at any two points (Baker and Oxborough 2003).

8. Fluorescence induction and electron transport— Dividing F_q' by F_m' gives the PSII photochemical efficiency under actinic light. F_q'/F_m' is an extremely useful parameter since it provides an estimate of the quantum efficiency of photosynthetic electron transport (Genty et al. 1989). The use of either the MT or ST technique for estimating PSII photochemical efficiency is of key importance here. PQ redox activity and k_{PQ} can be altered according to the photon flux density delivered to PSII. The differences observed between F_m' and F_q'/F_m' between ST and MT are, therefore, a function of actinic PPFD (Suggett et al. 2003). The PSII photochemical efficiency under actinic light has also been expressed as Φ_p or Φ_{PSII}. This is not strictly a quantum yield and use of Φ should, perhaps, be avoided.

The response of algae to light involves changes in the rate constants and fluorescence parameters for PSII photochemistry. F_q'/F_m' is the product of two parameters, the PSII maximum efficiency, $(F_m' - F_o')/F_m' = F_v'/F_m'$ and the PSII efficiency factor, $(F_m'-F')/(F_m'-F_o') = F_q'/F_v'$ (Baker & Oxborough 2003),

$$\frac{F_m'-F'}{F_m'} = \frac{F_m'-F'}{F_m'-F_o'} \cdot \frac{F_m'-F_o'}{F_m'} \quad \textit{hence} \quad \frac{F_q'}{F_m'} = \frac{F_q'}{F_v'} \cdot \frac{F_v'}{F_m'}$$

F_q'/F_v' has been routinely called the photochemical quenching coefficient, qP. At relatively low actinic irradiances, F_q'/F_m' will be largely affected by changes in F_q'/F_v' as a result of changes in k_p and, therefore, F'. The maximum PSII efficiency will be roughly equivalent to that observed in the dark-adapted state. Under relatively high PPFDs, mechanisms are required to further down-regulate the amount of excitation energy delivered to PSII and thus prevent damage to reaction centres, for example, xanthophyll

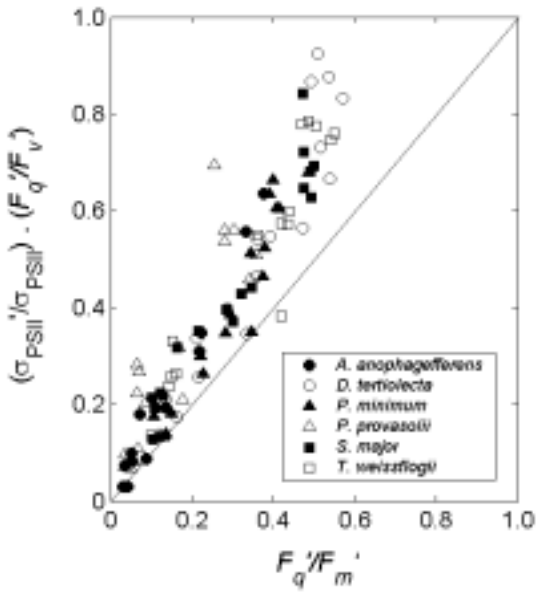

Figure 3. Comparison of the PSII photochemical efficiency calculated as F_q'/F_m' and ($\sigma_{PSII}'/\sigma_{PSII} \cdot F_q'/F_v'$) from the FRR fluorescence technique. Both variables are dimensionless. Measurements were made under actinic PPFDs of ~50, 200 and 600 µmol photons m^{-2} s^{-1} for six species of microalgae grown under 18, 80 and 300 µmol photons m^{-2} s^{-1}. Data are from Suggett and MacIntyre (unpubl.)

cycling, electron cycling around PSII and reaction centre deactivation. This results in an increase in k_h and a decrease in all fluorescence variables (see Schreiber et al. 1995b, Suggett et al. 2003). Irreversible damage to reaction centres may occur under excessive PPFD and/or low nutrient conditions and result in a decrease to rate constants for both photochemistry and those associated with quenching within the RCII itself (above). A variety of terms have been employed to quantify these various quenching processes (reviewed in Krause & Weis 1991, Maxwell & Johnson 2000) but may only be valid under certain conditions and/or rely on an accurate knowledge of corresponding dark-adapted values (Baker & Oxborough 2003).

Changes to the rate constant k_h under actinic light alter the effective functional antenna size. This enables another estimate of the PSII maximum efficiency to be obtained from FRR fluorometry as the ratio of the effective absorption in the light (σ_{PSII}') to that in darkness (σ_{PSII}) (Gorbunov et al. 2001). Use of σ_{PSII}': σ_{PSII} may be advantageous over F_v'/F_m', which may be subject to fluorescence quenching in the RCIIs themselves and hence underestimated (Fig. 3). In this case, the PSII photochemical efficiency is described as,

$$PSII\ photochemical\ efficiency = \frac{\sigma_{PSII}'}{\sigma_{PSII}} \cdot \frac{F_q'}{F_v'}$$

Both determinations of the PSII photochemical efficiency correspond with the quantum yield of PSII photochemistry, as mol e^- transferred per mol photons absorbed, and display a characteristic decline with light (Fig. 4). The dependence of the photon efficiency of photosynthesis on actinic irradiance (Suggett et al. 2001, 2003, Smyth et al. 2004) can be summarised as,

$$PSII\ PhotEff = \frac{\left[PSII\ PhotEff^{MAX} \cdot E_k\right] \cdot \left[1 - \exp(-E/E_k)\right]}{E}$$

where E_k is the light saturation parameter and $PSII\ PhotEff^{MAX}$ is the maximum predicted photochemical efficiency, calculated from either approach, and will be approximately equivalent to F_v/F_m. The same procedure can be applied for modelling changes in σ_{PSII} with light. This light-response model of the photochemical efficiency provides an E_k determination directly from the measured parameter and is preferable to an E_k determination from the light-response of the ETR (see Laws et al. 2002 and below).

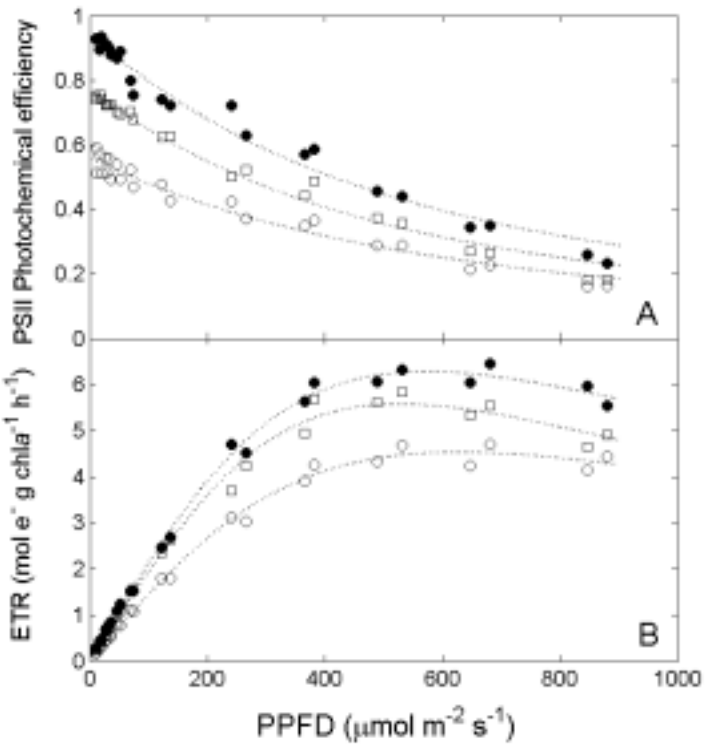

Figure 4. Light-response of (A) PSII photochemical efficiency (dimensionless) and (B) ETR (mol e- g chl*a*$^{-1}$ h^{-1}). PSII photochemical efficiencies are determined as F_q'/F_m' for the FRR (○) and PAM (□) and ($\sigma_{PSII}'/\sigma_{PSII} \cdot F_q'/F_v'$) for the FRR (●); ETRs are calculated as (PPFD · σ_{PSII} · n_{PSII} · F_q'/F_m' · 0.0243) for the FRR (○) and as (PPFD · a^{chl}_{PSII} · F_q'/F_m' · 0.0243) PAM (□) and as (PPFD · [σ_{PSII} · n_{PSII}] · [$\sigma_{PSII}'/\sigma_{PSII}$ · F_q'/F_v'] · 0.0243) for the FRR (●). Lines indicate PSII photochemical efficiency (Suggett et al. 2001, 2003) and ETR (Platt et al. 1980) light-response models fit to the data. All measurements were made simultaneously on *Prorocentrum minimum* grown under 50 µmol photons m^{-2} s^{-1} (Suggett et al. 2003).

The product of the PSII photochemical efficiency and the actinic PPFD is used to calculate the relative rate of electron transfer (Kromkamp and Forster 2003). However, this approach is not a satisfactory description of the photosynthetic potential. The absolute rate of electron transfer, ETR, is calculated with additional knowledge of the rate of light absorption specific to PSII, a_{PSII},

$$\text{ETR} = \text{PPFD} \cdot a_{PSII} \cdot \textit{PSII photochemical efficiency}$$

FRR fluorescence provides a direct measure of light absorption per unit PSII reaction centres (σ_{PSII}). Therefore, a combination of FRR measurements alone allows at least two equations for determining the absolute rate of electron transport through functional PSII (Gorbunov et al. 2001),

$$\text{ETR}^{RCII} = \text{PPFD} \cdot \sigma_{PSII} \cdot [\sigma_{PSII}'/\sigma_{PSII} \cdot F_q'/F_v'] \cdot 21.683$$
$$\text{ETR}^{RCII} = \text{PPFD} \cdot \sigma_{PSII} \cdot F_q'/F_m' \cdot 21.683$$

Where ETR^{RCII} is the RCII-specific rate of electron transfer (mol e- mol RCII^{-1} h^{-1}), PPFD is the photosynthetically active photon flux density (μmol photons m^{-2} s^{-1}) and the factor 21.683 converts seconds to hours, μmol e- to mol e- and $Å^2$ quanta^{-1} to m^2 mol RCII^{-1}. Knowledge of the photosynthetic unit size of PSII, n_{PSII} (mol RCII mol chla^{-1}), enables calculation of the ETR on a per unit-chlorophyll*a* basis,

$$\text{ETR}^{chl} = \text{PPFD} \cdot \sigma_{PSII} \cdot n_{PSII} \cdot [\sigma_{PSII}'/\sigma_{PSII} \cdot F_q'/F_v'] \cdot 21.683$$
$$\text{ETR}^{chl} = \text{PPFD} \cdot \sigma_{PSII} \cdot n_{PSII} \cdot F_q'/F_m' \cdot 21.683$$

Where ETR^{chl} is the chlorophyll*a*-specific rate of electron transfer (mol e- mol chla^{-1} h^{-1}). Further modifications to this equation will enable ETR may be per unit cell or per unit volume The biophysical absorption term can be replaced using bio-optical measures of light absorption by PSII where one is unable to measure n_{PSII} and/or σ_{PSII} (Suggett et al. 2003, 2004). This is almost certainly the case with other commercially available fluorescence induction techniques

The light-response of either ETR (Fig. 4) can be described analogously to photosynthesis-light response curves measured from more conventional techniques such as ^{14}C uptake or O_2 evolution. Following Platt et al. (1980),

$$\mathrm{ETR} = \mathrm{ETR}' \cdot \left(1 - \exp\left(-\alpha \cdot \mathrm{E}/\mathrm{ETR}'\right)\right) \cdot \left(\exp\left(-\beta \cdot \mathrm{E}/\mathrm{ETR}'\right)\right)$$

$$\mathrm{ETR}^{\max} = \mathrm{ETR}' \cdot \left(\alpha/\alpha+\beta\right)\left(\beta/\alpha+\beta\right)^{\beta/\alpha}$$

where ETR^{max} is the maximum rate of electron transport, α is the initial slope and β is the degree of photoinhibition of the ETR-light (E) response. ETR′ is the light saturated ETR that would be observed in the absence of photoinhibition. A variety of alternative models have been proposed and are discussed elsewhere (Aalderink & Jovin 1997, Gilbert et al. 2000).

9. Fluorescence induction and photosynthesis— Oxygen evolution is the direct result of PSII photochemistry and the action spectra of both fluorescence and oxygen evolution are very similar suggesting they share a common photochemical reaction (see Falkowski & Raven 1997). However, the yield of O_2 evolved per e^- transferred through PSII must be known in order to obtain O_2 productivity rates directly from ETRs. In all cases, the maximum yield of O_2 from each electron transfer step through PSII ($1/k$ and is equal to 0.25 mol O_2 (mol e^-)$^{-1}$) is assumed. Using $1/k$, it is possible to modify the above ETR algorithms,

$$P\mathrm{O}_2 = \mathrm{PPFD} \cdot \sigma_{\mathrm{PSII}} \cdot \mathrm{n}_{\mathrm{PSII}} \cdot 1/k \cdot [\sigma_{\mathrm{PSII}}'/\sigma_{\mathrm{PSII}} \cdot F_q'/F_v'] \cdot 21.683$$

$$P\mathrm{O}_2 = \mathrm{PPFD} \cdot \sigma_{\mathrm{PSII}} \cdot \mathrm{n}_{\mathrm{PSII}} \cdot 1/k \cdot F_q'/F_m' \cdot 21.683$$

Where PO_2 is the chlorophyll (or RCII)-specific gross rate of O_2 evolution (mol O_2 mol chla^{-1} (or mol RCII^{-1}) h^{-1}). Studies have shown that fluorescence-based estimates of O_2 productivity are routinely higher than independently measured rates of O_2 production for phytoplankton (Table 2). The actual difference between techniques varies significantly between investigations and reflects a number of factors: (1) deviation of $1/k$ from 0.25 mol O_2 (mol e^-)$^{-1}$ (2) inaccurate independent measurements of gross O_2 evolution (3)

inaccurate determination of the PSII quantum yield or a^{chl}_{PSII} (Flameling & Kromkamp 1998, Suggett et al. 2001, 2003). Firstly, cycling of electrons may act to reduce the photon efficiency of O_2 evolution whist maintaining the PSII photochemical efficiency. Secondly, the majority of comparisons to date have measured O_2 using polargraphic O_2 electrodes. This technique may under estimate gross O_2 evolution where photorespiration or the Mehler Reaction consumes O_2 intracellularly. Finally, possible theoretical inaccuracies in calculating the PSII quantum yield may depend on the use of ST versus MT protocols and reaction centre versus antenna fluorescence quenching and are discussed in previous sections. The potential practical inaccuracies are considered in Sections B and C. All these factors may operate according to the species in question or physiological status of a given sample. Therefore, interpretations and inter-comparisons are more complicated when based on natural samples.

Of greater importance to many aquatic studies is determination of algal

Investigation	Method		Approximate Observations
	Fluorescence	Production	
Kolber & Falkowski (1993) [a]	PP	^{14}C	$FRR(O_2) = 0.5\text{-}2 \cdot {}^{14}C$
Boyd et al. (1997) [a]	PP	^{14}C	$FRR(O_2) = 0.3\text{-}1.5 \cdot {}^{14}C$
Suggett et al. (2001) [a]	FRR	^{14}C	$FRR(O_2) = 0.5\text{-}2 \cdot {}^{14}C$
		O_2	$FRR(O_2) = 1\text{-}1.5 \cdot O_2$
Moore et al. (2003) [a]	FRR	^{14}C	$FRR(O_2) = 1\text{-}4 \cdot {}^{14}C$
Suggett et al. (2003) [b] *	FRR	$^{18}O_2$	$FRR(O_2) = 1\text{-}2 \cdot {}^{18}O_2$
Raateoja et al. (2004) [a]	FRR	^{14}C	$FRR(O_2) = 1\text{-}4 \cdot {}^{14}C$
Smyth et al. (2004) [a]	FRR	^{14}C	$FRR(O_2) = 0.6\text{-}1.2 \cdot {}^{14}C$
Flameling & Kromkamp (1998) [b] *	PAM	O_2	$PAM(O_2) = 6\text{->}50 \cdot O_2$
Hartig et al. (1998) [b]	PAM	^{14}C	$PAM(O_2) = 6\text{->}50 \cdot {}^{14}C$
Gilbert et al. (2000) [a]	PAM	^{14}C	$PAM(O_2) = 18\text{->}50 \cdot {}^{14}C$
Morris & Kromkamp (2003) [b]	PAM	O_2	$PAM(O_2) = 6\text{-}7 \cdot O_2$

Table 2. Summary of investigations that have compared fluorescence-based estimates of productivity (O_2) with independent measurements of O_2 evolution or ^{14}C uptake for phytoplankton. Data are taken from investigations that have estimated fluorescence-based productivity from *absolute* rates of electron transport (and assuming 0.25 mol O_2 evolved $(mol\ e^-)^{-1}$). Both single turnover (PP: Pump and Probe; FRR: Fast Repetition Rate) and multiple turnover (PAM: Pulse Amplitude Modulation) fluorescence based estimates are included. [a] signifies determinations on natural samples; [b] signifies determinations from individual cultures species; * signifies additional studies where both production estimates have been divided by a^{chl}_{PSII} to compare PSII quantum yields.

productivity in terms of C-fixed rather than O_2 evolved. Several studies have directly compared ETR-based estimates of O_2 and rates of ^{14}C uptake (Table 2). The differences observed between ETR-based estimates of O_2 and ^{14}C uptake are greater than those observed between ETR-based estimates of O_2 and O_2 evolution. This is not surprising since an additional number of pathways may intercept ETR-based energy prior to C-uptake than O_2 evolution (Flameling & Kromkamp 1998, Suggett et al. 2003, Behrenfeld et al. 2004). Again, the significance of these pathways is not well understood. What is clear is that considerable efforts must be made to understand the energy partitioning by individual phytoplankton species in order to use fluorescence as a routine proxy of productivity *per se*.

B. Bench-top fluorescence measurements

Discrete observations are highly desirable since they provide a more complete understand than instantaneous fluorescence signals recorded *in situ*. In practice, fluorometers are simply arranged on a bench-top to accommodate individual cuvettes (Suggett et al. 2003, 2004) or flow-through cells (Laney et al. 2001). Algal material is removed from natural or laboratory growth conditions and exposed to controlled environmental stimuli thus placing actual limits within which photochemistry can operate in nature. The following section details fluorescence methodologies that have been employed in this manner.

1. ***Sample Collection—*** Discrete fluorescence measurements require algal material that is dark-adapted. Specifically, non-photochemical pathways must be released from the transient but cumulative affects of daytime light exposure to enable two or more samples to be directly comparable. Samples are typically dark-adapted for at least 30-45 minutes (Falkowski et al. 1986, Falkowski & Kolber 1995, Babin et al. 1996); however, true dark-adaptation may require hours (Krause & Weis 1991, Kolber & Falkowski 1993). Relaxation of non-photochemical quenching has two phases: an initial fast phase (½ time 5-15 minutes) and a slower, secondary phase (½ time 1-3 hours) (Kolber & Falkowski 1993). These two phases characterise the re-establishment of trans-thylakoid pH and repair of damaged PSII reaction centres, respectively, to pre-illuminated conditions. Therefore, the actual time required for complete dark-adaptation will be dependent upon the degree to which exposure differs from ambient growth conditions and the pathways that are available for de-excitation.

● Removal of water samples from the environment immediately alters the conditions to which algae are routinely exposed. Therefore, it is crucial to maintain samples under controlled conditions and to process samples as quickly as possible. Water is collected from the surface or from depth using CTD rosettes. All samples must be collected into darkened containers that have been rinsed clean of previous samples or, if new, plastic residues. Darkened tubing should be used to funnel water between containers to prevent transient exposure to bright light, in particular where water is collected from depth.

Finally, samples should be maintained in the darkened containers and at in-water temperatures until processed.

● The minimum period of dark acclimation will be dependent upon the time required to collect and transfer samples to the laboratory. Therefore, logistical constraints may dictate the actual period of dark acclimation that is chosen. A set period of dark-acclimation for all samples may give rise to inconsistencies within and between data sets and some distinction may be required where measurements are made in the dark but are not truly dark-acclimated (Maxwell & Johnson 2000). Alternatively, samples should be repeatedly measured over a period of time to determine the level of dark-acclimation that has been achieved. A relatively easy approach that can be standardised is to obtain discrete water samples at dawn for immediate use.

● For discrete fluorescence measurements, a sample is introduced into a cell following dark-acclimation and maintained at the growth temperature. The cell may be individually cooled, for example using a temperature control probe (Suggett et al. 2003), or the entire fluorometer and cell may be maintained in a temperature-controlled environment. In either case, the instrument should be characterised (section B.4) at the temperature at which it is operated.

2. ***FRR Fluorescence measurements—*** Fluorescence measurements in darkness characterise the physiological 'potential' for processing light energy. Fluorescence under actinic light characterises the actual extent that light energy is passed to photochemistry or dissipated as heat. This information is collected in one of two ways, (1) Discrete measurements at an actinic PPFD that is equivalent to the growth PPFD and (2) fluorescence-light (F-E) response curves. The first approach is performed using the same methodology as discrete dark measurements except that the cell is illuminated with the appropriate PPFD (see below). The second approach enables a more complete description of the photosynthetic capability of algae and is analogous to photosynthesis-irradiance (P-E) curves from conventional techniques, such as ^{14}C uptake or O_2 evolution. Two types of F-E response protocols have been employed: (1) rapid F-E response curves

(White & Critchley 1999) and (2) steady state F-E response curves (Suggett et al. 2003). Both protocols measure fluorescence under a gradient of increasing actinic PPFDs but differ in the period of illumination at each actinic PPFD.

● To avoid 'dark effects' (section A.6), true dark FRR fluorescence acquisitions should be made under very weak actinic light and separated by 1-second intervals (Suggett et al. 2003, 2004). Dark-adapted values of F_v/F_m and σ_{PSII} correspond well with maximum values obtained by modelling the relationship between F_q'/F_m' and σ_{PSII}' and light (described in section A.8) suggesting that F_v/F_m and σ_{PSII} could be estimated from F-E curves.

● Typically, rapid F-E curves deliver light for periods of 10-30 seconds whilst steady state F-E curves deliver light for periods of 3-5 minutes. Fluorescence yields, σ_{PSII} and F_v/F_m alter upon immediate exposure to light but subsequently settle to a new and constant level, the steady state. This trend presumably reflects the capacity of the donor and acceptor reactions of photochemistry to optimise linear electron flow following a change in PPFD. The actual period of actinic light for steady state curves will depend upon the difference in PPFD between light steps and the light harvesting capabilities of individual algae. Additional environmental factors including nutrient stress and in

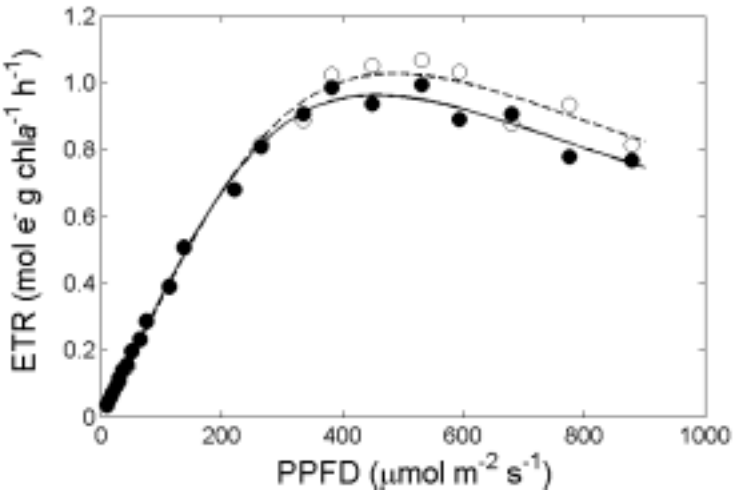

Figure 5. ETR calculated from FRR measurements of F_q'/F_m' (ETR = PPFD · a^{chl}_{PSII} · F_q'/F_m' · $3.6 \cdot 10^{-3}$). F_q'/F_m' is obtained after 30 seconds (closed circles) or after 4 minutes (open circles) to yield 'steady state' and 'rapid' F-E curves. The alternative determinations yield different ETR^{max} and E_k, the light saturation parameter, when fit with the Platt et al. (1980) light-response model (solid and broken lines, respectively) This example is from *Thalassiosira weissflogii* grown under 80 µmol photons m^{-2} s^{-1}.

particular temperature are also likely to play a role. However, the minimum time can be determined from continual monitoring of fluorescence throughout the experiment, for example, the minimum fluorescence (F') from the PAM fluorometer (section A.7) or the initial EM: EX from the FRR fluorometer (section B.5). Therefore, the two types of F-E curve differ in the fluorescence yields that are measured and the F-E that is observed (Fig. 5).

● Both approaches yield a useful description of intracellular light energy dissipation following changes in actinic PPFD. Rapid F-E curves follow the capability of PSII photochemistry to respond to rapid increases in light. Steady state F-E curves follow the optimal PSII photochemistry to which cells are acclimated. As such, steady state F-E curves more closely resemble conventional P-E experiments. In any case, care should be taken when comparing data where F-E light responses have been generated using different protocols. Similarly, comparisons between F-E and P-E will be complicated by the different time scales used to generate the light response (MacIntyre et al. 2002).

● Rapid F-E curves are considered practical since samples are manipulated for a short period of time (5-10 minutes). Steady state F-E curves require a period of ~1 hour depending on the number of PPFDs chosen. In either case, the sample must be stirred regularly to avoid settling of cells or aggregates and hence a potential change in the absolute fluorescence yield. The sample temperature should be monitored.

● Illumination for all F-E curves is delivered from an actinic source positioned at right angles to the optics receiving the fluorescence signal. PPFDs are increased using neutral density filters or, in the case of LEDs, changing the duty cycle. The PPFDs should be measured prior to every F-E curve inside the sample cell and in line with the optical arrangement for excitation and emission. An additional band pass filter may be desirable for 'white' actinic sources to (1) reduce the amount of red light contamination to the PMT (2) reduce the amount of heating to the sample throughout experimentation. These actinic sources will not match the actinic spectra that samples are exposed to for growth in the laboratory or in nature. Therefore, actinic PPFDs must be spectrally corrected to

yield a more accurate description of the F-E relationship (appendix III). A short dark break of 5-10 acquisitions is required for FRR F-E curves between light levels to reduce interference to the fluorescence signal for determination of σ_{PSII}'. As such, rapid F-E curves may not be suitable for an FRR F-E protocol.

3. *Blank Corrections*— For any fluorescence signal, corrections need to be made to account for instrument and sample blanks in order to confidently interpret fluorescence induction measurements (Cullen & Davis 2003, Laney 2003). Amongst the factors that contribute to instrument blanks are electronic offsets (baseline), electronic noise and biases (the 'instrument response function') and signal quality (scatter). These sources of error are inherent to the build of a given instrument and can be affected according to the temperature at which the fluorometer electronics operate. However, these sources are relatively easy to correct for (Laney 2003). A sample blank may arise from fluorescence of coloured dissolved organic matter (CDOM) present in the sample, stray light scattered into the detector either from the ambient (actinic) light source or the excitation light source, as well as fluorescence from detritus ("dead" chlorophyll).

● Chlorophyll *a* standards (Sigma) or pigment extracts in acetone and de-ionised water can be used to determine the instrument response function (IRF) and scatter function, respectively (Suggett et al. 2003, 2004, Moore et al. 2005). Alternatively, Rhodamine B solution may be used for the IRF (Laney 2003). IRF solutions should be made to obtain maximum signal but so as not to saturate the PMT (section B.5). At least 200 acquisitions should be made for each gain and chamber according to the protocols employed for the corresponding sample collection. Processing the sample data with and without the IRF signal can yield significantly different values of modelled variables, for example the effective absorption cross section (σ_{PSII}, Fig. 6). The IRF will vary between instruments and gain settings (Laney 2003).

● The CDOM fluorescence may account for a significant proportion of the total fluorescence yield in low chlorophyll*a* waters. Specifically, a background CDOM fluorescence yield that is not associated with active (variable) fluorescence is inherent to

the minimum fluorescence measurement (F_o, F'). Consequently, fluorescence ratios, such as the photochemical efficiency may be affected by the blank,

Photochemical efficiency = $(F_{max}\text{-}F_{min})/F_{max}$
where $F_{min} = F_{min}$ (active phytoplankton) + F_{min} (background)

CDOM fluorescence blanks can be measured on sample filtered through a 0.2 μm pore size sieve filter or a 0.4 μm (nominal) pore size glass fibre filter (Moore et al. 2003, 2005; Suggett et al. 2003, 2004; Cullen and Davis, 2003). Gravity filtration of a water sample is required to prevent physical disruption of active cells and thus an overestimation of the detritus within a sample blank. In additional, filtration should be performed under minimum actinic light to prevent degradation and fluorescence

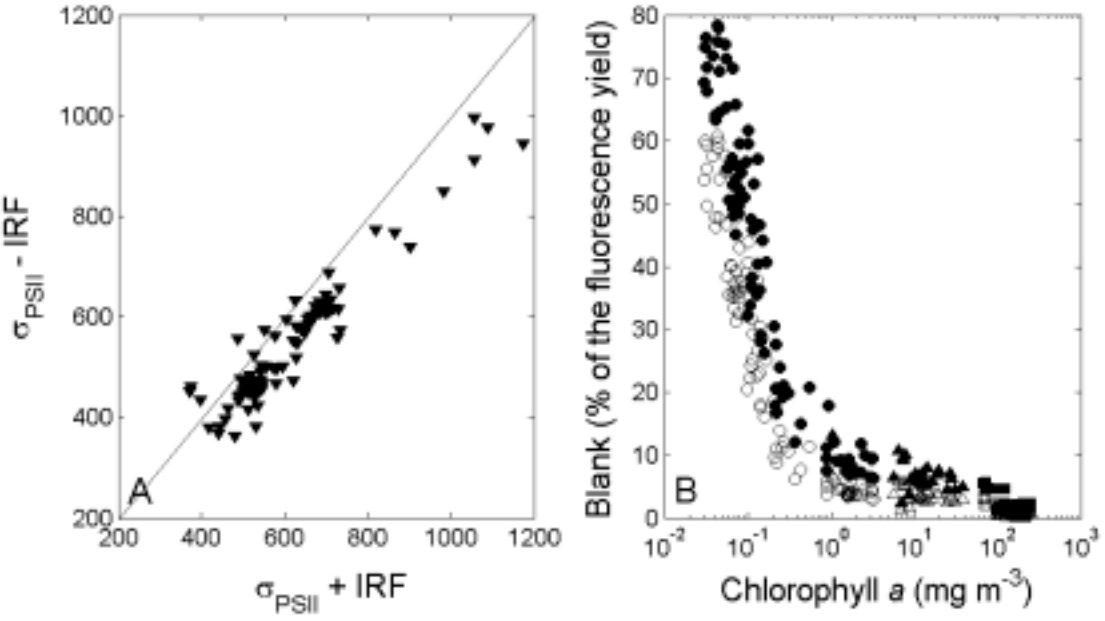

Figure 6. (A) The effective absorption cross-section (σ_{PSII}, Å^2 quanta^{-1}) determined with and without the instrument response function (IRF) using v4 software (Sam Laney). σ_{PSII} – IRF ≈ 5-15% σ_{PSII} + IRF The IRF was determined from 200 acquisitions of chlorophyll*a* standard in acetone (Sigma) and using the same protocol/instrument temperature as *in situ* data collection. Data for this example was collected with the FRR set to a gain of 1 and moored in the English Lake District 2003 (Suggett, unpubl.). (B) Relationship between the percentage of the fluorescence yield that is attributable to the CDOM blank versus the chlorophyll *a* concentration of the original sample. Data are taken from the Atlantic open ocean (circles, Moore unpubl.), the Lake District (triangles, Suggett unpubl.) and various batch cultures (squares, Le F'loch unpubl.). The % of the blank is determined from both maximum (F_m, open symbols) and minimum (F_o, closed symbols) fluorescence yields.

quenching within the CDOM fraction. Following this methodology, laboratory and field investigations have shown that algal biomass directly determines the proportion of the active fluorescence signal that can be accounted for from the CDOM blank (Fig. 6). However, this association is likely to be modified by the trophic status of a given community.

● In addition to correcting for a sample blank, calculations of absolute photosynthetic electron transfer rates may require corrections for fluorescence that arises from pigments that are not involved in photosystem II photochemistry. This includes fluorescence that arises from photosystem I, as well as fluorescence that arises from phycobilipigments in crytomondas, rhodophytes and cyanobacteria. We return to these points latter in the methods.

4. ***Bench-top FRR protocols—*** Two single turnover (ST) protocols are delivered by FRR fluorometry, termed saturation and relaxation. The saturation protocol delivers a series of flashlets, which cumulatively close the majority of PSII reaction centres and induces a rise from minimum to maximum fluorescence. A model describing the kinetics of Q_A reduction is then fitted to the fluorescence rise (Kolber et al. 1998) to determine the F_o (F'), F_m (F_m'), F_v/F_m (F_q'/F_m'), σ_{PSII} (σ_{PSII}') and ρ (ρ′) (section B.5).

● Of key importance to any fluorescence measurement is maximising the signal without saturating the detector. The choice of gain should be made such that the dark-acclimated emission (EM) to excitation (EX) ratio does not exceed a value of ~1.0-1.5. However, the actual value may depend upon the specific sensitivity of the PMT of any given instrument, and users should attempt to aim for dark-adapted EM: EX within 50-60% of the minimum PMT sensitivity at each gain. This is particularly important for subsequent light-response measurements since the EM: EX will increase once samples are exposed to actinic light. The EM: EX should be read real-time following each acquisition, for example, using the *verbose* mode of FAST^{tracka}. The minimum gain (lowest sensitivity) may saturate when used for assessment of laboratory cultures. In which case, neutral density filters can be placed over the optical windows of the detector. These filters

dampen the fluorescence signal but do not significantly alter the fluorescence induction curve or subsequent determinations of F_v/F_m (F_q'/F_m'), σ_{PSII} (σ_{PSII}'), ρ (ρ') or τ (τ') (Suggett, unpubl.).

• The maximum fluorescence yield should be obtained within 50-60% of the total number of flashlets in order to adequately resolve the variables from the model (Kolber et al. 1998, Laney 2003). However, algae with a small effective absorption cross-section (σ_{PSII}) exhibit a slower cumulative fluorescence rise than algae with a large σ_{PSII}. Therefore, it is important to either choose a single generalised saturation protocol that is appropriate for all species and physiological conditions or continually alter the saturation protocol. Use of a single generalised protocol is particularly advantageous for natural samples containing a mixture of species. Alteration of the length and frequency of each flashlet changes the rate at which the reaction centres close (Kolber et al. 1998, Laney 2003, Suggett et al. 2003). Custom-built systems can deliver a range of ST protocols within 120 µs (Kolber et al. 1998). In contrast, the fastest rate of closure of PSII reaction centres obtained from the commercially available FRR FAST^{tracka} is 280 µs (100 saturation flashes with the inter-flash delay of 2.8 µs; note, the flashlet duration is included in the inter-flash timing). We have found that this fastest FAST^{tracka} protocol represents the minimum requirement to yield a saturation plateau for cyanobacteria, which have the smallest cross sections (Suggett et al. 2004). Therefore, this saturation protocol has been employed routinely. However, protocols should be continually verified for each instrument or as modifications improve the rate at which flashlets can be delivered.

• The relaxation protocol is only of use for discrete samples (or sedentary organisms, such as corals) since the protocol time likely exceeds the period that any given parcel of water is exposed to the optical windows. The FRR FAST^{tracka} relaxation protocol is set to deliver 20, 1.1 µs flashlets with an inter-flash interval of 50 µs. This yields a relaxation protocol lasting 2 ms. However, the fitting software (section B.5) may require modification in order to obtain a reliable estimate of electron transport from Q_A and through the plastoquinone pool (Moore, unpubl.).

5. ***Processing bench-top FRR measurements—*** EM and EX signals for the saturation and relaxation flashlets are downloaded to a PC. Subsequent EM: EX will depend upon how well the signal: noise has been optimised from the choice of gain and potential signal scatter or interference from the light (quality and quantity). The Kolber-Falkowski-Prasil model (Kolber et al. 1998) describing kinetics of Q_A reduction and subsequent re-oxidation is then fitted to the FRR fluorescence induction curves (EM: EX).

● Improving the signal: noise can be achieved by merging a sequence of EM: EX acquisitions before processing (model fitting). Alternatively, a sequence of fluorescence variables may be averaged after processing. Convergence of the model fit is increased when EM: EX acquisitions are merged, in particular when the variable fluorescence and effective absorption cross-sections are small or the signal: noise has not been optimised from the instrument settings (Fig. 7). Therefore, we routinely merge EM: EX acquisitions prior to processing. Consideration must be made before data collection for (1) the

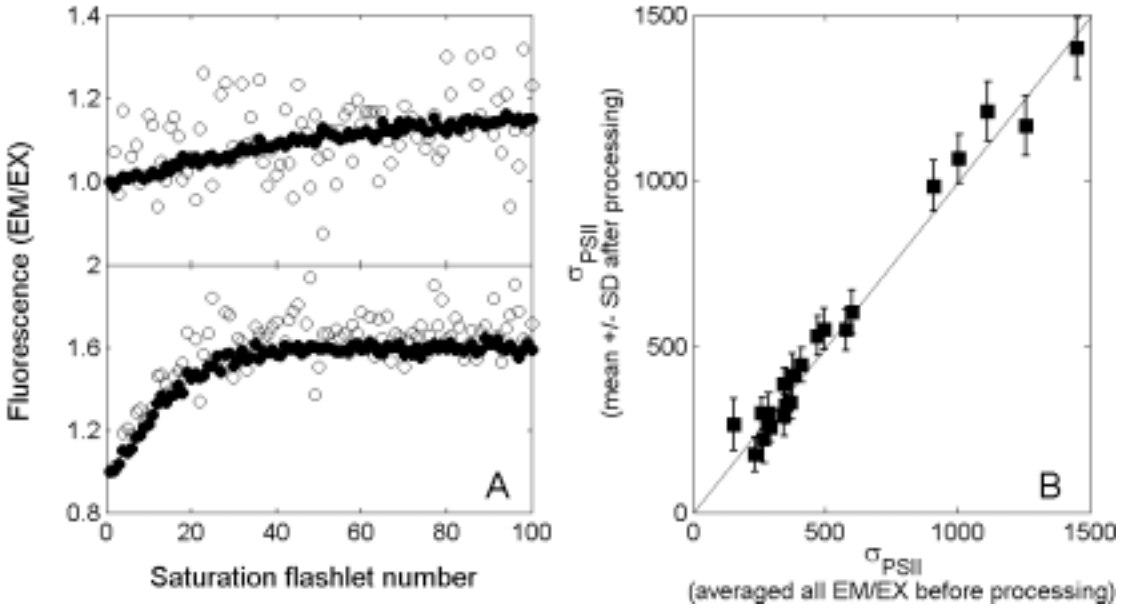

Figure 7. (A) Examples of FRR fluorescence saturation transients to which the Kolber-Prasil-Falkowski model is fitted. Open circles are from an individual acquisition whilst closed circles are from the average 15 consecutive acquisitions. The upper panel is for *Synechococcus spp*. 1479/9 and the lower panel is for *P. provasolii* (Suggett et al. 2004). (B) Comparison of σ_{PSII} determinations from fitting the Kolber-Prasil-Falkowski model to acquisitions that have been averaged before (x-axis) and after (y-axis) processing.

temporal resolution that can be sacrificed (2) replicates for post processing assessment of physiological variables. These considerations will inevitably increase the number of acquisitions and determine the data collection strategy, in particular given inevitable constraints of field sampling campaigns.

● Several versions of software are available to fit the Kolber-Prasil-Falkowski model to the saturation and relaxation fluorescence transients obtained from FRR fluorometry. The choice of processing software has received recent detailed attention (Laney 2003) and is beyond the scope of this manual. All software versions are available from the *FRRF users group* (http://picasso.oce.orst.edu/ORSOO/FRRF/).

C. *In situ* fluorescence measurements

Instantaneous measurements of primary productivity *in situ* are highly desirable since they avoid artefacts associated with incubations of discrete water samples (Laws et al. 2002). Variable fluorescence is widely recognised as a potential tool for routinely assessing phytoplankton productivity *in situ*. However, investigations to date have frequently been limited by the sampling strategies employed and hence the quality of the variable fluorescence data and subsequent ability to estimate ETRs. Sampling using submersible active fluorometers should take into account a number of potential weaknesses in deployment strategy and subsequent data processing. Here we consider sampling and acquisition protocols that can enable the collection of useful and consistent variable fluorescence data for phytoplankton across a range of aquatic environments.

1. Instrument maintenance and deployment—The current version of the FAST^{tracka} FRRf was originally designed as a profiling instrument and has thus been optimised for *in situ* deployment. Currently the FRRf has been deployed on standard oceanographic CTD systems (e.g. Suggett et al. 2001, Moore et al. 2003, 2005, Smyth et al. 2004), on optical profiling rigs (e.g. Smyth et al. 2004) or stand alone frames (Raateoja et al. 2004), on towed undulating vehicles (e.g. Moore et al. 2003; Allen et al. 2003) and on stand alone moorings (Suggett et al., in prep.). To facilitate *in situ* deployment the FRRf is contained within a titanium pressure case. Power can be provided using a battery pack (e.g. Suggett et al. 2001, Moore et al. 2003; Smyth et al. 2004) or through an interface with other instruments (e.g. Allen et al. 2003). In the latter case, interface with a CTD package or underwater data acquisition system eliminates the need for battery recharging and can allow near-real time data monitoring (Allen et al. 2003). The instrument can also be interfaced with a 2π PAR sensor and pressure sensor (Chelsea Instruments).

● Regardless of the deployment strategy, care should be taken to ensure that the optical windows on the instrument are kept clean. The instrument is configured with two sampling areas, one is typically exposed to ambient irradiance, while the second is frequently shaded using a purpose built chamber (Fig. 8). Optical surfaces are typically

cleaned between deployments using a damp smooth-fibred tissue. Optics should be frequently checked for scratches, the presence of which might require a new characterisation of the instrument response to be performed.

● If data collected from the un-shaded sample area are required, care must be taken to avoid additional shading of the instrument optics during deployment. In particular, the instrument should be located towards the top of any deployment package to prevent shading from other objects including, for example, the CTD or water sampling bottles (Fig. 8). Additional care should be taken to prevent shading of the instrument package by the ship (Moore et al. 2005; Smyth et al. 2004). Ideally the ship should be aligned such that the sun is falling on the side over which deployment occurs (Fig. 8). Clearly this may not be possible under certain sea conditions. Provided the PAR sensor has been located

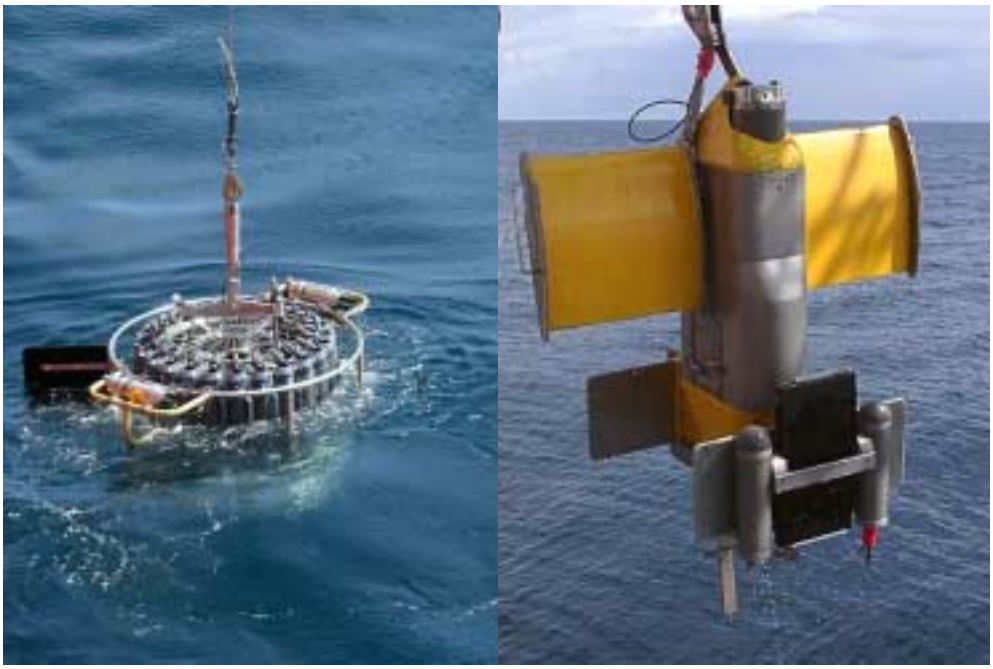

Fig. 8 Pictures of *in situ* FRRf deployments. *Left,* Two FAST^{tracka} FRRfs deployed on a CTD package. FRR fluorometers are situated at the top of the CTD package and external to the main frame in order to minimise shading of the optics during deployment. PAR sensors are also located at the top of the CTD rig. The ship has been aligned such that the CTD is deployed on the sunward side. *Right*, FAST^{tracka} FRRf deployed on a towed undulator Seasoar (Allen et al. 2002). Location of FRRf is not ideal as the nose and bridle of the tow body can shade the instrument optics. The sampling area exposed to ambient irradiance can be seen facing the camera. The purposefully shaded sampling area is behind and flushed using two U-shaped pipes.

close to the FAST^{tracka} FRR optical head, vertical irradiance profiles can be inspected to ascertain whether ship shading has occurred (Moore et al. 2005).

● The current FAST^{tracka} FRR suffers from ambient light problems in the near surface (Moore et al. 2003; Laney, 2003; Raatoja et al 2004). Specifically, chlorophylla concentration and thus fluorescence yields are low and are measured against a high backgound flux of red light. These ambient 'red' photons in the near surface may have wavelengths overlapping the detection band of the FRR FAST^{tracka}. Also, these photons can be scattered and detected by the PMT, swamping the fluorescence signal. As a single PMT is shared between the two sample areas, degradation of the fluorescence signal is not only limited to measurements made in the area exposed to ambient irradiance (Fig. 9). These problems are absent at depth, the long wavelength photons having been rapidly attenuated. Data should be inspected and the near surface degraded signals removed. The amount of data lost is likely to depend on the ambient light level and the optical properties of the water body. In coastal waters we have routinely disregard data collected between the surface and around 2-5m depending on water clarity (Moore et al. 2003). Data that do not pass further quality control procedures are also removed (Fig. 9). In clear oceanic waters this problem is likely to result in the rejection of data even deeper into the water column.

● For vertical deployments on CTD systems or using similar platforms, the profiling speed may be dictated by external constraints. Due to the potential for high levels of noise within data collected *in situ* and hence the potential requirement for data averaging (see above section B.5) slow profiling speeds and hence highly resolved profiles are preferable. This is of particular importance when attempting to construct the light response of fluorescence parameters (F-E) using the *in situ* irradiance gradient (e.g. Smyth et al. 2004). As a result of the exponential nature of the light field, recovering data at enough resolution in high light may be particularly problematic (Fig. 9). The resolution obtainable for any given profiling speed will depend on trade-offs between signal averaging and acquisition.. Additionally it may be necessary to profile more slowly through any strong gradient regions. Under ideal conditions, for example in a fully mixed

water column (Fig. 9), the natural phytoplankton population can be assumed to have a uniform physiology with depth, hence the use of the natural light gradient for deriving irradiance dependent variability is reasonably well justified. In contrast for strongly

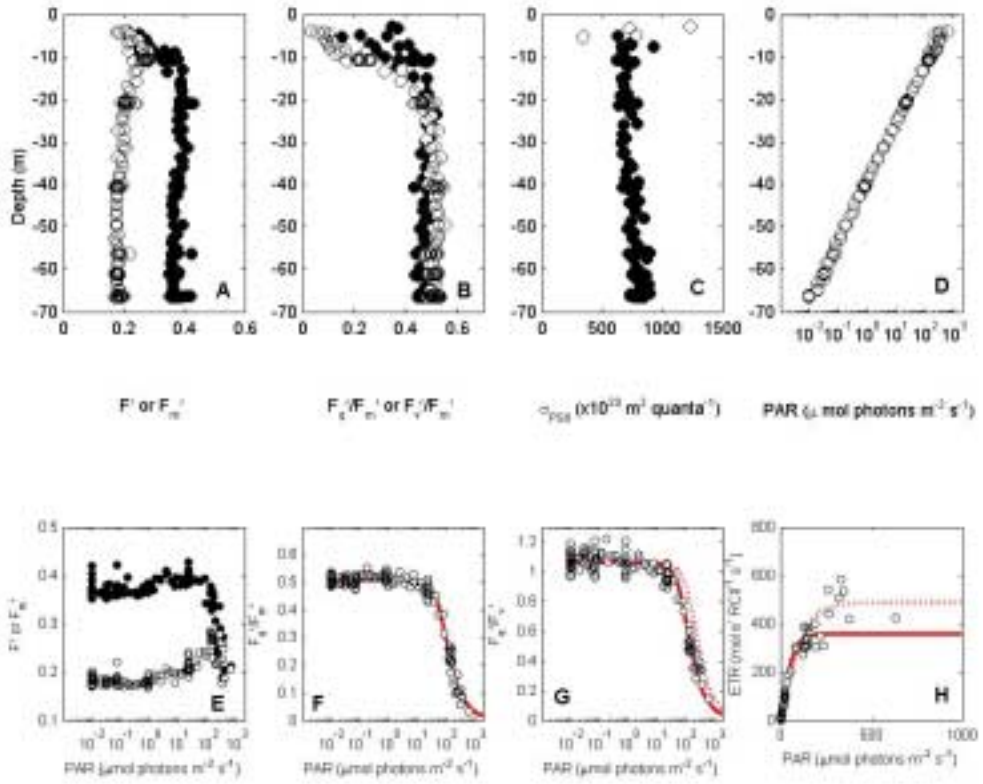

Fig. 9 Example of fluorescence parameters measured *in situ* using a vertically profiled submersible FAST^{tracka} FRR. These data were collected under near optimal conditions in a fully mixed water column (water depth 77m) with a relatively high pigment biomass (~0.5 µg Chl l^{-1}), during a sunny cloud free period. Panels A-D present vertical profiles of (A) F' (open symbols) and F_m' (closed), (B) F_q'/F_m' (open) and F_q'/F_m' (closed), (C) σ_{PSII}', measured in the shaded area of the submersible instrument. All data and quality controlled data (closed symbols) collected deeper than 3m are shown. Data failing quality controlled checks, where error in fitted value of σ_{PSII}' > 20% are indicated by open symbols. (D) Irradiance (PAR) showing a clear exponential decrease with depth. Panels E-F, fluorescence-irradiance relationships. (E) F' (open symbols) and F_m' (closed) vs PAR, (F) F_q'/F_m' vs PAR, red lines indicates fit to equation in section A.8. (G) F_q'/F_v' v PAR, solid line indicates fit to equation in section A.8. (H) reaction centre specific ETR = σ_{PSII}' F_q'/F_v'E vs PAR. Solid line indicates the expected relationship estimated from fit to data in (G), dotted line indicates fit of ETR vs E data to equation in section A.8. Note dotted line in (G) is transposed from fit of dotted line in (H) demonstrating a poorer fit of the yield irradiance relationship when ETR vs E is used. For FRRf data this likely results from larger errors in F_q'/F_v' at high irradiance being given large weightings once multiplied by E. Generally better estimates of water column ETR will result from fitting the yield-irradiance relationship (G) rather than the rate irradiance relationship (H), (Laws et al. 2002).

stratified waters, where a marked deep chlorophyll maximum is frequently observed, this assumption may require testing. Additionally deep chlorophyll maximum layers can be narrow, in extreme cases only a few meters wide (e.g. Sharples et al. 2001), complicating adequate sampling of this population with a profiled FAST^{tracka} instrument.

• For stand-alone deployments when the instrument is not interfaced with a CTD package or other system (e.g. Allen et al. 2003), data is recorded internally on a flashcard. This data can then be downloaded following the deployment. Download can take some considerable time. To minimise the possibility of large quantities of data being lost it is recommended that the download operation be performed as frequently as practically possible.

• Sampling rates from towed vehicles are best set at the maximum as towing tends to result in a high effective vertical profiling rate. Again care should be taken to ensure the shading of instrument optics is minimal (Fig. 8). Obtaining useful well resolved and meaningful vertical profiles using towed instruments remains challenging (Allen et al. 2003).

• Sampling rates for moored instruments will be dictated by the length of deployment, battery life and, if data is being stored internally, the memory capacity. There are no published reports of operating a FAST^{tracka} FRR fluorometer from a mooring. Suggett et al. (in prep.) have successfully maintained an FRRf on a mooring in the English Lake District for 6 weeks collecting data continuously at hourly intervals. This data collection rate was indeed compromised by the battery life and the potential data loss during download (ie. the amount of material that was stored on the memory card). Ultimately, these limitations were the result of the frequency with which the FRRf could be visited for servicing. It is clear that data streaming and power supply methods for moored acquisition can be improved. However, instrument maintenance and collection of water samples for instrument blanking (and data interpretation) must still be performed at regular intervals thus compromising a fully autonomous mode of operation.

2. Data acquisition— Acquisition of useful variable fluorescence data from *in situ* profiles is largely determined by an optimal deployment strategy (section C.1) combined with an optimal instrument set-up. Settings required for *in situ* profiling will be dictated to a large extent by the parameters required (Table 1). Thus, for example, if the difference between variables measured with and without the influence of photochemical quenching is not of interest, then only one of the FAST^{tracka} FRRf 'chambers' need be activated. Bearing in mind such potential differences required in special cases, the following outlines typical settings that we have found to produce reasonable data for *in situ* profiles in a variety of oceanographic contexts (Fig. 9).

- Choice of saturation and relaxation protocols should take account of all the points noted for discrete (benchtop) protocols mentioned above (section B). The saturation protocol is typically chosen to deliver 100 1.1 μs flashes with the inter-flash delay of 2.8 μs. This protocol has been found to adequately saturate the variable fluorescence response in the majority of natural phytoplankton populations sampled from estuarine, through coastal to oligotrophic oceanic waters. In order to obtain well resolved averaged flashlet data, the internal averaging option is frequently used (e.g. Moore et al. 2003). Additional averaging can also be performed during data processing after download (section B.5).

- The relaxation protocol is not considered useful for *in situ* profiling. Any protocol sufficiently long to resolve all but the fastest fluorescence decay transients will likely exceed the period that any given parcel of water is exposed to the optical windows. Hence it is unlikely that accurate measures of τ_{Qa} can be recovered from *in situ* data, although we currently know of no rigorous test of this supposition.

- The consideration of CDOM blank effects is as important with *in situ* data as with data collected on discrete samples (section B.4). However in the case of a profiled or towed *in situ* deployment, correction for blank effects may be considerably more difficult than in the laboratory. As stated by Cullen and Davis (2003) 'the appropriate blank…is seawater from which phytoplankton have been removed, under the same ambient irradiance as

encountered through the vertical profile'. Temperature can also potentially influence the fluorescence signal (Cullen and Davis, 2003; Laney, 2003). Adequate accounting for blank effects *in situ* is thus a considerable challenge. Filtered seawater blanks from samples collected throughout the water column and run on identical instrument settings to *in situ* measurements can potentially constrain the magnitude of the errors (Fig. 6B). Preferably these measurements should also be made at a number of differing irradiances (Cullen and Davis, 2003). Alternatively, fluorescence signals collected from deeper in the water column below the surface layer have been used as a method for blank collection. Recognising the absence of a truly rigorous test of the extent to which these protocols introduce errors in the derived fluorescence parameters, we recommend that filtered sea-water blanks from appropriate depths in surface waters be used whenever possible.

● Users should be aware of the fluorescence parameters that are particularly susceptible to blank fluorescence effects and the reasons for this. Measurements of both F_0 (hence also F', F_0') and F_m (F_m') will all be influenced by a blank offset (Fig. 6B). Thus due to the nature of the derivation F_v/F_m (F_q'/F_m', F_v'/F_m') are highly dependent on the magnitude of the CDOM blank. In contrast, F_v should be insensitive to a constant offset in both F_0 and F_m and hence F_q'/F_v' is also likely to be insensitive. Additionally parameters such as σ_{PSII} (σ_{PSII}') that are derived from rates of change of fluorescence transients should be less sensitive to CDOM blanking effects. Again such assumptions require further rigorous testing, although data have confirmed the insensitivity of σ_{PSII} to blank effects (Moore and Suggett, unpublished).

● Again, similar to discrete samples, IRFs should also be run on chlorophyll *a*, pigment extracts or other fluorophores to account for any non-linearity in instrument response. Measurements of IRFs over the range of temperatures encountered *in situ* would further allow for assessment of potential thermal effects (Laney, 2003). Characterisation of instrument response should be performed as fully as possible for every set of instrument settings (e.g. gain) used to collect data (Laney, 2003).

● The FAST^{tracka} FRR has a limited sensitive range at any given gain setting. For *in situ* measurements the choice of the gain setting will depend on the pigment concentration within the natural population to be sampled. For fixed gain settings an initial estimate of the appropriate range can be made from independent fluorescence or extracted pigment measurements. Pigment concentrations may change during an *in situ* deployment. For example moored deployments may span a range of different conditions at any one location. Additionally sub-surface chlorophyll maxima can contain much higher pigment concentrations than surface waters (e.g. Sharples et al. 2001). Optimal FRRf measurements from surface and sub-surface waters may therefore require different gain settings. To account for these situations, the FAST^{tracka} has an autoranging facility. Autoranging can be employed successfully provided that profiling is made sufficiently slowly, the rate of data acquisition is high and that pigment biomass does not change sharply in the water column. In contrast, we have found that the time response of the gain change can be inadequate to account for the sharp gradients in pigment biomass sometimes encountered in both coastal and open ocean waters. Autogain thresholds can be modified in an attempt to pre-empt changes in fluorescence that may result in saturation of the PMT and ultimately a loss of data. However, even such modification requires an instrument-response time and thus may not be suitable for water columns that have extremely complex (variable) physical-biological structure. If possible we therefore prefer to deploy multiple instruments on a single deployment package to span the range of gains required to obtain optimal data within the environment sampled (Fig. 8). Clearly this option may not be available to many users. An alternative for vertical profiling at a site may be to perform multiple deployments with the same instrument at different gain ranges. Users should carefully inspect their data to ascertain whether such measures are necessary. In general a gain setting that is too low (i.e. lower sensitivity) is preferable to one which is too high. Variable fluorescence data that saturates the PMT will not allow accurate calculation of physiological parameters, whereas data collected at too low a sensitivity, despite being more noisy, may still be useful for the recovery of parameters (section B.5).

● In general data should be inspected as soon as possible after deployment in order that any problems can be identified and, if necessary, changes in deployment strategy or instrument settings made.

3. In situ ETR determinations— One of the major uses of the FAST^{tracka} FRR has been the calculation of electron transport rates and hence the estimation of photosynthesis *in situ* (Gorbunov et al. 2001, Suggett et al. 2001, Moore et al. 2003, Raateoja et al. 2004, Smyth et al. 2004). Assuming *in situ* active fluorescence data have been collected in a near optimal manner, a number of issues should still be addressed in the calculation of electron transport rates. A number of researchers have collected vertical profiles of fluorescence data and then applied algorithms to estimate ETR or PO_2 (section A.8) (e.g. Kolber and Falkowski, 1993; Boyd et al. 1997; Suggett et al. 2001; Raateoja et al. 2004; Smyth et al. 2004). All have used slightly different methods and assumptions, complicating comparisons between studies. Here we make a number of recommendations for protocols, however, as with many of the other suggestions, further work is required.

● As a result of the potential for both vertical and diel physiological variability, care should be taken in estimating the daily electron transport rate from a single profile of variable fluorescence parameters. Repeated profiles at a location over the course of a day are more likely to yield robust estimates of daily ETR (Suggett et al. 2001; Smyth et al. 2004).

● Direct estimation of light limited electron transport rates is possible using *in situ* active fluorescence data (e.g. Smyth et al. 2004). Conversely, as the quality of fluorescence data degrades towards near surface high light regions (section B.2), direct estimation of maximal electron transport rates is problematic. Robust estimates of water column or daily electron transport can be obtained by estimating the light limited rate and then applying a model describing how the quantum yield of electron transport (see section A.8) behaves at high light (Smyth et al. 2004). Additionally, as quantum yield measurements degrade in the surface, fitting the quantum yield vs irradiance curve rather than the ETR vs irradiance profile will avoid placing large weighting on potentially

inaccurate values of ETR in the surface (Fig. 9) (see Laws et al. 2002). Even assuming near surface high ETRs could be accurately measured, fitting the quantum yield vs. irradiance response is still preferable for generating accurate estimates of water column ETR from a limited number of profiles (Laws et al. 2002).

● Several additional factors will affect estimates of daily ETR, in particular, spectral variability between light sources (e.g. Suggett et al. 2001, 2004; Moore et al. 2003; Raateoja et al. 2004). Additionally, scaling relative rates of ETR to water column rates requires a number of assumptions or additional measurements. Such 'corrections' add significant complexity to the FRR technique, at least in terms of obtaining FRR fluorescence-based ETR or productivity estimates that are not only consistent across environments and phytoplankton communities but also across independent investigations. We have outlined two of the most crucial methods; that of the photosynthetic unit size of PSII, n_{PSII}, and the spectral correction of light absorption from different light sources, in appendices II and III.

Appendix I. Active fluorescence parameterisation

	Authors	Kromkamp & Forster 2003 Baker & Oxborough 2003 Baker et al. 2001		PAM					Pump & Probe; FRRF			
				Maxwell & Johnson 2000	Hartig et al. 1998 Flameling & Kromkamp 1998	Schreiber et al. 1993, 1995a, b	van Kooten & Snel 1990	Genty et al. 1989	Gorbunov et al. 2000, 2001	Kolber et al. 1998	Kolber & Falkowski 1993	Falkowski et al. 1986 Kolber et al. 1988
Dark		F_o	Minimum fluorescence	F_o	F_o	F_o	F_o	ϕF_o	F_o	F_o	F_o	F_p
		F_m	Maximum fluorescence	F_m	F_m	F_m	F_m	ϕF_m	F_m	F_m	F_m	F_s
		F_v	Variable fluorescence ($F_m - F_o$)	F_v	F_v	F_v	F_v	-	F_v	F_v	F_v	-
		F_v/F_m	Photochemical efficiency	F_v/F_m	F_v/F_m	F_v/F_m	-	-	F_v/F_m	F_v/F_m	$\Delta\phi_m$	-
Actinic Light		F'	Steady-state fluorescence at any point	F_t	F, F_s	F	F_s	ϕF_s	F'	-	F'	-
		F_o'	Minimum fluorescence	F_o'	F_o'	F_o'	F_o'	ϕF_o	F_o'	-	F_o'	-
		F_m'	Maximum fluorescence	F_m'	F_m'	F_m'	F_m'	ϕF_m	F_m'	-	F_m'	-
		F_v'	Variable fluorescence ($F_m' - F_o'$)	-	F_v'	-	F_v'	ϕF_v	F_v'	-	F_v'	-
		F_q'	Difference of F_m' and F' ($F_m' - F'$)	-	-	ΔF	-	$\Delta\phi_F$	$\Delta F'$	-	-	-
		F_q'/F_m'	Photochemical efficiency	Φ_{PSII}	Φ_P	Φ_{PSII}	-	$\Delta\phi_F/\phi_{Fm}$	$\Delta F'/F_m'$	-	-	-

Appendix II. Converting reaction centre normalised determinations of ETR

FRR fluorometry directly yields ETRs specific to the number of PSII reaction centres available for photochemistry (Gorbunov et al. 2001, section A.8). However, RCII normalised rates of algal productivity cannot be placed in the true context of phytoplankton biomass since the concentration of RCIIs *in situ* is not measured. The photosynthetic unit size of PSII, n_{PSII} (mol RCII mol chl*a*$^{-1}$, Table 1), can be used to convert ETR in mol e^- mol RCII^{-1} h^{-1} to both an ETR in mol e^- g chl*a*$^{-1}$ h^{-1} and a potential O_2 productivity, PO_2, of mol O_2 g chl*a*$^{-1}$ h^{-1}. Chlorophyll specific ETR can then be readily converted to absolute ETR as a result of the straightforward methods available for measurement of chlorophyll *in situ*. n_{PSII} can be routinely measured on laboratory grown cultures (Falkowski et al. 1981, Dubinsky et al. 1986, Suggett et al. 2003, 2004). In contrast, n_{PSII} is typically approximated for natural samples using an assumed constant and an RCII 'functionality factor' (Kolber and Falkowski, 1993, Babin et al. 1996, Suggett et al. 2001, Moore et al. 2003, Raateoja et al. 2004). This indirect approximation can result in considerable error when compared with actual measurements of n_{PSII} (Suggett et al. 2004).

● The photosynthetic unit size is routinely determined from the O_2 evolved by ST saturating flashes delivered at a range of flash frequencies (Falkowski et al. 1981, Dubinsky et al. 1986, Suggett et al. 2003, 2004). Algal suspensions are maintained in a commercially available oxygen chamber. A Clarke-type electrode is used to measure the O_2 yields whilst a custom built lighting system delivers ST flashes. The O_2 flash yield measurements should be repeated following addition of $NaHCO_3$ to correct for any affect of photorespiration (Dubinsky et al. 1986, Suggett et al. 2004).

● The algal suspensions used must contain a chlorophyll *a* concentration that is 100-1000 fold greater than that found in nature to be within the sensitivity of the commercially available O_2 electrodes. Even dense laboratory cultures must be pre-concentrated. This is performed by gravity filtration (or using a very gentle and controlled vacuum, such as from a hand pump) onto GF/C or nucleopore filters. The cells are gently re-suspended or

washed from the filters into a 5-10 ml of filtrate. Typically, 150-250 ml of laboratory culture and 5-10 litres of natural samples must be pre-concentrated. PSII photochemical efficiencies should be measured before and after concentration to ensure that PSII reaction centres have not been significantly damaged form the concentration procedure.

• Limited sensitivity of the O_2 electrode ensures that the technique is not currently appropriate for routine determination of n_{PSII} in the field (Moore et al. subm.). However, improvements to the sensitivity of O_2 sensors may overcome this limitation. The O_2 electrode does not provide a strict measure of gross O_2 evolution. Therefore, flash induced O_2 evolution may be more accurately measured from $^{18}O/^{16}O$ analyses in future studies. For direct approximations of carbon assimilation, it may be possible to determine n_{PSII} on a mol C per mol RCII basis by substituting flash induced O_2 evolution with flash induced ^{14}C uptake measurements. Furthermore, Suggett et al. (2004) have recently proposed an alternative method whereby n_{PSII} could be determined *in situ* from optical and biophysical absorption measurements. None of the above alternative n_{PSII} approaches have yet been attempted for natural samples

Appendix III. Spectral Corrections

Quantification of light absorption under actinic light must be corrected to the actual spectral quality of light to which samples are exposed in nature. Specifically, σ_{PSII} from the FRR fluorometer is measured by excitation from blue LEDs (λ_{max} = 478 nm) (Fig. 10). In reality, the underwater spectra will be composed of a mixture of colours (Fig. 10) and result in a different rate of excitation of PSII and hence σ_{PSII}. The same applies when determining the light response of photochemistry, which inherently contains a function of light absorption specific to the actinic light source. The magnitude of the correction required will depend on (1) the wavelengths of light most readily absorbed by particular

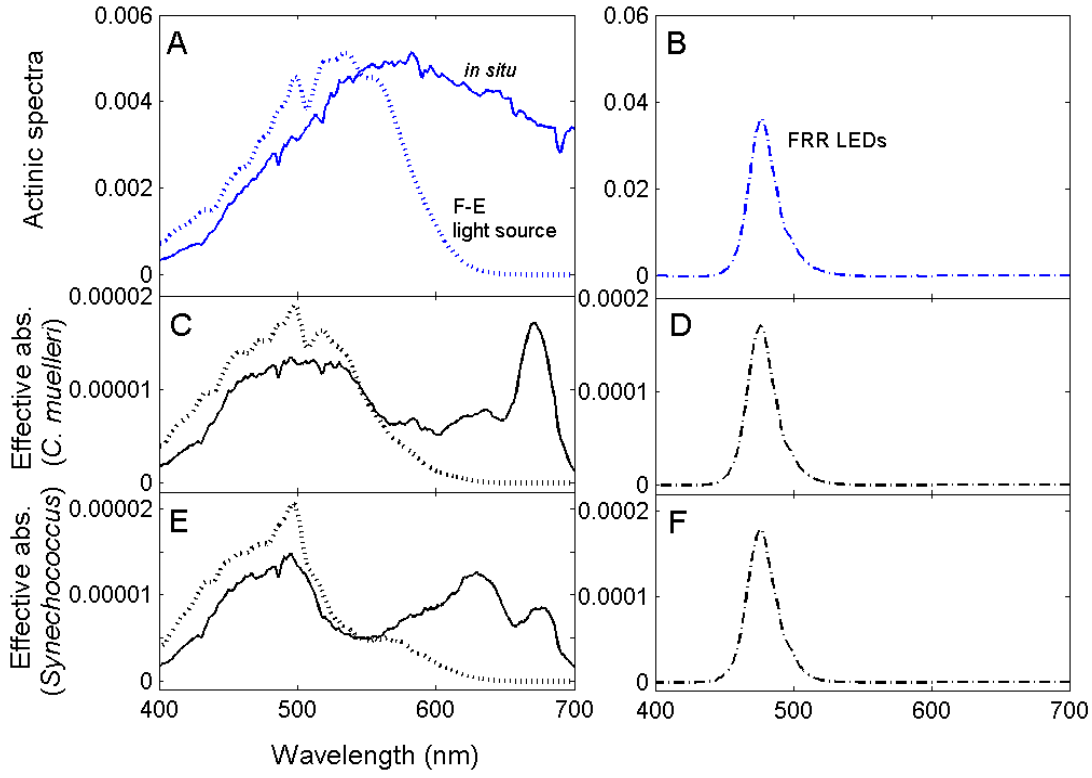

Figure?. Actinic spectra from (A) a light source used for fluorescence-light (F-E) response experiments and *in situ* (this example is from 1m in the English Lake District, Suggett, unpubl.) and (B) from the FRR fluorometer LEDs. Effective absorption spectra of diatom *C. muelleri* (C and D) and cyanophyte Synechococcus spp. 1479/9 *(*E and F) when excited from the three different actinic sources. In these examples, the effective absorption coefficients are the sum of the absorption from 400-700 nm. Note that the FRR excitation is confined to the 'blue' and yields relatively a narrow band of high effective absorption. The actual coefficient from the FRR spectra is approximately twice that from the F-E light source or *in situ* spectra.

species and (2) the degree of difference in light quality between the actinic source and underwater (Suggett et al 2001, Moore et al. 2003, Raateoja et al. 2004).

- Light absorption by any particular light source can be calculated as,

$$\frac{\sum_{400}^{700} a^{chl}_{(\lambda)} \cdot E_{(\lambda)}}{\sum_{400}^{700} E_{(\lambda)}} \quad \delta\lambda$$

where E is the PPFD of the actinic light source and a^{chl} is the chlorophyll-a specific light absorption of the sample. Ideally, F_{730} or a^{chl}_{PSII} should be used instead of a^{chl} since these describe the light absorption that is actually used for PSII photochemistry (Suggett et al. 2004). To compare spectral differences in light absorption from two or more light sources, E must be equal, for example, setting the area under all spectra to 1. These calculations thus yield an absorption coefficient specific to each light source. These coefficients are used to adjust the rate of light absorption from an actinic source to the rate of light absorption from the actual light experienced *in situ* (Fig. 10).

References

Aalderink R.H., and R., Jovin. 1997. Estimation of the photosynthesis/irradiance (P/I) curve parameters from light and dark bottle experiments. J. Plankton Res. 19 (11): 1713-1742.

Allen, J., V. Cornell, C.M. Moore, N. Crisp, and J. Dunning, 2002 Operational oceanography using the new SeaSoar undulator. Sea Technology 43 35-40

Babin, M., A. Morel, H. Claustre, C. Bricaud, Z. Kolber, and P. G. Falkowski. 1996. Nitrogen- and irradiance-dependent variations of the maximum quantum yield of carbon fixation in eutrophic, mesotrophic and oligotrophic marine systems. Deep Sea Res. 43 (8): 1241-1272.

Baker, N.R., and K. Oxborough. 2003. Chlorophyll fluorescence as probe of plant photosynthetic productivity. In Chlorophyll fluorescence: A signature of photosynthesis (Papageorgiou, C.G., & Govindgee, A.D., editors). Kluwer Academic Press, Dordrecht.

Baker, N.R., K. Oxborough., T. Lawson, and J.I.L. Morison. 2001. High resolution imaging of photosynthetic activities of tissues, cells and chloroplasts in leaves. J. Expt. Botany. 52 (SI): 615-621.

Barranguet C., and J.C. Kromkamp. 2000. Estimating primary production rates from photosynthetic electron transport in estuarine microphytobenthos. Mar. Ecol. Prog. Ser. 204: 39-52.

Behrenfeld, M. J., and Z. S. Kolber. 1999. Widespread iron limitation of phytoplankton in the South Pacific Ocean. Science 283: 840-843.

Behrenfeld, M. J., O. Prasil, M. Babin, and F. Bruyant. In search of a physiological basis for covariations in light-limited and light-saturated photosynthesis. J. Phycol. 40: 4-25

Berhardt, K., and H.W. Trissl. 1999. Theories for kinetics and yields of fluorescence and photochemistry: how, if at all, can different models of antenna organization be distinguished experimentally? Biochim. Biophys. Acta. 1409(3): 125-142.

Bidigare, R. R., M. E. Ondrusek, J. H. Morrow, and D. A. Kiefer. 1990. In vivo absorption properties of algal pigments. SPIE 1302 (Ocean Optics X): 289-302.

Boyd, P.W., J. A. Aiken, and Z. S. Kolber. 1997. Comparison of radiocarbon and fluorescence based (pump and probe) measurements of phytoplankton photosynthetic characteristics in the northeast Atlantic Ocean. Mar. Ecol. Prog. Ser., 149: 215-226.

Butler, W.L. 1978. Energy distribution in the photochemical apparatus of photosynthesis. Ann. Rev. Plant Physiol. 29: 345-378.

Casper-Lindley, C., and O. Bjorkman. 1998. Fluorescence quenching in four unicellular algae with different light-harvesting and xanthophylls-cycle pigments. Photosynth. Res. 56: 277-289.

Cullen, J.J., and R.E. Davies. 2003. The blank can make a big difference in oceanographic measurements. Limnol. Oceanogr. Bull. 12 (2): 29-35.

Dijkman, N.A., B.M.A. Kroon. 2002. Indications for chlororespiration in relation to light regime in the marine diatom *Thalassiosira weissflogii*. J. Photochem. Photobiol. B. 66: 179-187. FALKOWSKI, P.G. & RAVEN, J.A. (1997). Aquatic Photosynthesis. Blackwell, USA.

Dubinsky, Z., P. G. Falkowski, and K. Wyman. 1986. Light harvesting and utilisation by phytoplankton. Plant Cell Physiol. 27(7): 1335-1349.

Falkowski, P.G., and D.A. Kiefer. 1985. Chlorophyll a fluorescence in phytoplankton: relationship to photosynthesis and biomass. J. Plankton Res. 7 (5): 715-731.

Falkowski, P. G., and Z. S. Kolber. 1995. Variations in chlorophyll fluorescence yields in phytoplankton in the worlds oceans. Austr. J. Plant Physiol. 22: 341-355.

Falkowski, P. G., Z. S. Kolber, and Y. Fujita. 1988. Effect of redox state on the dynamics of photosystem II during steady-state photosynthesis in eukaryotic algae. Biochim. Biophys. Acta. 933: 432-443.

Falkowski, P. G., T. G. Owens, A. C. Ley, and D. C. Mauzerall. 1981. Effects of growth irradiance levels on the ratio of reaction centres in two species of marine phytoplankton. Plant Physiol. 68: 969-973.

Falkowski, P. G., and J. A. Raven.1997. Aquatic Photosynthesis. Blackwell, USA.

Falkowski, P.G., K. Wyman, A.C. Ley, and D.C. Mauzerall. 1986. Relationship of steady state photosynthesis to fluorescence in eucaryotic algae. Biochim. Biophys. Acta. 849: 183-192.

Finazzi, G., F. Rappaport, A. Furia, M. Fleischmann, J-D. Rochaix, F. Zito and G. Forti. 2002. Involvement of state transitions in the switch between cyclic and linear electron flow in *Chlamydomonas reinhardtii*. EMBO reports 3 (3): 280-285.

Flameling, I.A., and J. Kromkamp. 1998. Light dependence of quantum yields for PSII charge separation and oxygen evolution in eukaryotic algae. Limnol. Oceanogr. 43 (2): 284-297.

Genty, B., J-M. Briantais, and N.R. Baker. 1989. The relationship between the quantum yield of photosynthetic electron transport and quenching of chlorophyll fluorescence. Biochim. Biophys. Acta. 990: 87-92.

Gilbert, M., A. Domin, A. Becker, and C. Wilhelm. 2000. Estimation of primary productivity by chlorophyll *a* in vivo fluorescence in freshwater phytoplankton. Photosynthetica 38 (1): 111-126.

Gorbunov, M. Y., Z. S. Kolber, M. P. Lesser, and P. G. Falkowski. 2001. Photosynthesis and photoprotection in symbiotic corals. Limnol. Oceanogr. 46 (1): 75-85.

Gorbunov, M. Y. and P. G. Falkowski. 2004. Fluorescence Induction and Relaxation (FIRe) technique and instrumentation for monitoring photosynthetic process and primary production in aquatic ecosystems. In *Photosynthesis: Fundamental Aspects to Global Perspectives* (Ed. A. van der Est and D. Bruce). Allen Presss.

Hartig, P., K. Wolfstein, S. Lippemeier, and F. Colijn. 1998. Photosynthetic activity of natural microphytobenthos populations measured by fluorescence (PAM) and ^{14}C-tracer methods: a comparison. Mar. Ecol. Prog. Ser. 166: 53-62.

Hofstraat, J. W., K. Rubelowsky, and S. Slutter. 1992. Corrected fluorescence excitation and emission spectra of phytoplankton: toward a more uniform approach to fluorescence measurements. J. Plankton Res. 14: 625-636.

Horton P., A.V. Ruban, and R.G. Waters. 1996. Regulation of light harvesting in green plants. Ann. Rev. Plant Physiol. Plant Mol. Biol. 47: 655-685.

Jacobson, B. S., and D. Branton. 1977. Plasma membrane: rapid isolation and exposure of the cytoplasmic surface by use of positively charged beads. Science 195: 302-304.

Johnsen, G., and E. Sakshaug. 1993. Bio-optical characteristics and photoadaptive responses in the toxic and bloom-forming dinoflagellates *Gyrodinium aureolum, Gymnodinium galatheanum* and two strains of *Prorocentrum minimum*. J. Phycol. 29: 627-642.

Kautsky, H., W. Appel, and H. Amman. 1960. Chlorophyll fluorescenz und kohlensaure assimilation. Biochem. Z. 332: 277-292.

Koblížek M., D. Kaftan, and L. Nedbal. 2001. On the relationship between non-photochemical quenching of chlorophyll fluorescence and the photosystem II harvesting efficiency. A repetitive flash fluorescence induction study. Photosynth. Res. 68: 141-152.

Kolber, Z. S., and P. G. Falkowski 1993. Use of active fluorescence to estimate phytoplankton photosynthesis in situ. Limnol. Oceanogr. 38 (8): 1646-1665.

Kolber, Z. S., O. Prášil, and P. G. Falkowski. 1998. Measurements of variable chlorophyll fluorescence using fast repetition rate techniques: defining methodology and experimental protocols. Biochim.Biophys.Acta 1367: 88-106.

Krause, G.H, and E. Weis 1991. Chlorophyll fluorescence and photosynthesis: the basics. Ann. Rev. Plant Physiol. Plant Mol. Biol. 42: 313-349.

Kromkamp, J. C., and R. M. Forster. 2003. The use of variable fluorescence measurements in aquatic ecosystems: differences between multiple and single turnover measuring protocols and suggested terminology. Eur. J. Phycol., 38: 103-112.

Laney, S. R. 2003. Assessing the error in photosynthetic properties determined by fast repetition rate fluorometry. Limnol. Oceanogr. 48 (6): 2234-2242.

Laney, S.R. R.M. Letelier, A. Desiderio, and M.R. Abbott. 2001. Measuring the natural fluorescence of phytoplankton cultures. J. Atm. Oceanic Tech. 18: 1924-1934.

Laws, E., E. Sakshaug, M. Babin, Y. Dandonneau, P. Falkowski, R. Geider, L. Legendre, A. Morel, M. Sondergaard, M. Takahashi, and P. J. le B. Williams. 2002. Photosynthesis and primary productivity in marine ecosystems: Practical aspects and application of techniques. JGOFS report 36, July 2002.

Lutz, V. A., S. Sathyendranath, E. J. H. Head, and W. K. W. Li. 1998. Differences between in vivo absorption and fluorescence excitation spectra in natural samples of phytoplankton. J. Phycol. 34: 214-227.

Lutz, V. A., S. Sathyendranath, E. J. H. Head, and W. K. W. Li. 2001. Changes in the in vivo absorption and fluorescence excitation spectra with growth irradiance in three species of phytoplankton. J. Plankton Res. 23(6): 555-569.

MacIntyre, H.L., T.M. Kana, T. Anning, and R.J. Geider. 2002. Photoacclimation of photosynthesis irradiance response curves and photosynthetic pigments in microalgae and cyanobacteria. J. Phycol. 38: 17-38.

Maxwell, K., and G.N. Johnson. 2000. Chlorophyll fluorescence – a practical guide. J. Expt. Botany, 51: 659-668.

Mitchell, B. G., A. Bricaud, K. Carder, J. Cleveland, G. Ferrari, R. Gould, M. Kahru, M. Kishino, H. Maske, T. Moisan, L. Moore, N. Nelson, D. Phinney, R. Reynolds, H. Sosik, D. Stramski, S. Tassan, C. Trees, A. Weidemann, J. Wieland, and A. Vodacek. 2000. Determination of spectral absorption coefficients of particles, dissolved material and phytoplankton for discrete water samples, p. 125-153. In G. S. Fargion and J. L. Mueller [eds.], Ocean optics protocols for satellite ocean color sensor validation, Revision 2, NASA Technical Memorandum-2000-209966, USA.

Morris E.P., and J.C. Kromkamp. 2003. Influence of temperature on the relationship between oxygen- and fluorescence-based estimates of photosynthetic parameters in a marine benthic diatom (*Cylindrotheca closterium*). Eur. J. Phycol. 38: 133-142.

Moore, C. M., D. J. Suggett, P. M. Holligan, J. Sharples, E. R. Abraham, M. I. Lucas, T. P. Rippeth, N. R. Fisher, J. H. Simpson, and D. J. Hydes. 2003. Physical controls on phytoplankton physiology and production at a shelf sea front: a fast repetition rate fluorometer based field study. Mar. Ecol. Prog. Ser. 259: 29-45.

Moore, C.M., M.I. Lucas, R. Sanders and R. Davidson. 2005. Basin-scale variability of phytoplankton bio-optical characteristics in relation to bloom state and community structure in the Northeast Atlantic. Deep Sea Res. *In press*

Neori, A., M. Vernet, O. Holm-Hansen, and F. T. Haxo. 1988. Comparison of chlorophyll far-red and red fluorescence excitation spectra with photosynthetic oxygen action spectra for photosystem II in algae. Mar. Ecol. Prog Ser. 44: 297-302.

Parkhill, J-P., G. Maillet, and J.J. Cullen. 2001. Fluorescence-based maximal quantum yield for PSII as a diagnostic of nutrient stress. J. Phycol. 37: 517-529.

Platt, T., C.L. Gallegos, and W.G. Harrison. 1980. Photoinhibition of photosynthesis in natural assemblages of marine phytoplankton. J. Mar. Res. 38: 687-701.

Oxborough, K., and N.R. Baker. 1997. Resolving chlorophyll a fluorescence images of photosynthetic efficiency into photochemical and non-photochemical components – calculation of qP and F_v'/F_m' without measuring F_o'. Photosynth. Res. 54: 135-142.

Oxborough, K., A.R.M. Hanlon, G.J.C. Underwood, and N.R. Baker. 2000. *In vivo* estimation of the photosystem II photochemical efficiency of individual microphytobenthic cells using high-resolution imaging of chlorophyll *a* fluorescence. Limnol. Oceanogr. 45: 1420-1425.

Prasil, O., Z. Kolber, J.A. Berry, and P.G. Falkowski. 1996. Cyclic electron flow around photosystem II in vivo. Photosynth. Res. 48 (3): 395-410.

Raateoja, M., J. Seppälä, and H. Kuosa. 2004. Bio-optical modelling of primary production in the SW Finnish coastal zone, Baltic Sea: fast repetition rate fluorometry in case 2 waters. Mar. Ecol. Prog. Ser. 267: 9-26.

Sakshaug, E., A. Bricaud, Y. Dandonneau, P.G. Falkowski, D.A. Kiefer, L. Legendre, A. Morel, J. Parslow, and M. Takahashi. 1997. Parameters of photosynthesis: definitions, theory and interpretation of results. J. Plankton Res. 19 (11): 1637-1670.

Schatz, G.C., H. Brook, and A.R. Holtzwarth. 1988. A kinetic and energetic model for the primary processes in photosystem II. Biophys. J. 54:397-405.

Schreiber, U., C. Neubauer, and U. Schliwa. (1993). PAM fluorometer based on medium-frequency pulsed Xe-flash measuring light: A highly sensitive new tool in basic and applied photosynthesis research. Photosynth. Res. 36: 65-72.

Schreiber, U., C. Neubauer, and U. Schliwa. 1993. PAM fluorometer based on medium-frequency pulsed Xe-flash measuring light: A highly sensitive new tool in basic and applied photosynthesis research. Photosynth. Res., 36: 65-72.

Schreiber, U., H. Hormann, H., C. Neubauer, and C. Klughammer. (1995). Assessment of photosystem II photochemical quantum yield by chlorophyll fluorescence quenching analysis. Aust. J. Plant Physiol. 22: 209-220.

Suggett, D., G. Kraay, P. Holligan, M. Davey, J. Aiken, and R. Geider. 2001. Assessment of photosynthesis in a spring cyanobacterial bloom by use of a fast repetition rate fluorometer. Limnol. Oceanogr. 46 (4): 802-810.

Suggett, D.J., H. L. MacIntyre and R. J. Geider. Evaluation of biophysical and optical determinations of light absorption by photosystem II in phytoplankton. Limnol. Oceanogr.: Methods. 2: 316-332.

Suggett, D.J., K. Oxborough, N. R. Baker, H. L. MacIntyre, T. M. Kana, and R. J. Geider. 2003. Fast Repetition Rate and Pulse Amplitude Modulation chlorophyll *a* fluorescence measurements for assessment of photosynthetic electron transport in marine phytoplankton. Eur. J. Phycology 38 (4): 371-384.

Van Kooten, O., and J.F.H. Snel. 1990. The use of chlorophyll fluorescence nomenclature in plant stress physiology. Photosynth. Res. 25: 147-150

Vasiliev, I. R., Prášil, O., K. D. Wyman, Z. S. Kolber, K. A. Hanson Jr., J. E. Prentice, and P. G. Falkowski. 1994. Inhibition of PSII photochemistry by PAR and UV radiation in natural phytoplankton communities. Photosynth. Res. 42: 61-64.

Vernotte, C., A.L. Etienne, and J-M. Briantais. 1979. Quenching of the system II chlorophyll fluorescence by the plastoquinone pool. Biochim. Biophys. Acta. 545: 519-527.

White A.J., and C. Crtichley. 1999. Rapid light curves: a new fluorescence method to assess the state of the photosynthetic apparatus. Photosynth. Res. 59: 63-72.

Yaakoubd, B., R. Andersen, Y. Desjardins, and G. Samson. 2002. Contributions of the free oxidised and Q_B-bound plastoquinone molecules to the thermal phase of chlorophyll a fluorescence. Photosynth. Res. 74: 251-257.

Chelsea Technologies Group

55 Central Avenue
West Molesey
Surrey KT8 2QZ
United Kingdom
Tel: +44 (0)20 8481 9000
Fax: +44 (0)20 8941 9319
sales@chelsea.co.uk
www.chelsea.co.uk